



Test Plan for Wireless Device Over-the-Air Performance

CTIA 01.70 Measurement Uncertainty

Version 6.0.1

September 2023

© 2001 - 2023 CTIA Certification. All Rights Reserved.

Any reproduction, modification, alteration, creation of a derivative work, or transmission of all or any part of this publication ("Test Plan"), in any form, by any means, whether electronic or mechanical, including photocopying, recording, or via any information storage and retrieval system, without the prior written permission of CTIA Certification, is unauthorized and strictly prohibited by federal copyright law. This Test Plan is solely for use within the CTIA Certification Program. Any other use of this Test Plan is strictly prohibited unless authorized by CTIA Certification or its assigns in writing.

Use Instructions

All testing shall be performed in a CTIA Certification Authorized Test Lab and shall be initiated through one of the following methods:

1. By submitting a PTCRB or IoT Network Certified device certification request at <https://certify.ptcrb.com/>
2. By submitting an OTA Test Plan use request at <https://certify.ctiacertification.org/>

CTIA Certification LLC
1400 16th Street, NW
Suite 600
Washington, DC 20036

1.202.785.0081

programs@ctiacertification.org

ctiacertification.org/test-plans/

Table of Contents

Section 1	Introduction	8
1.1	Scope	8
1.2	Acronyms and Definition	8
Section 2	Treatment of Measurement Uncertainty Components	12
2.1	Mismatch	13
2.1.1	Special Requirement for SISO, Millimeter Wave	14
2.2	Cable Factor	14
2.3	Insertion Loss	15
2.4	Receiving Device	15
2.5	Signal Generator or Base Station Simulator	15
2.6	Network Analyzer	16
2.7	Amplifier	16
2.7.1	Gain	17
2.7.2	Mismatch	17
2.7.3	Stability	17
2.7.4	Linearity	17
2.7.5	Amplifier Noise Figure/Noise Floor	17
2.8	Reference Antenna	18
2.8.1	Gain Reference	18
2.8.2	Efficiency Reference	18
2.8.3	Unknown K factor	19
2.9	Measurement Distance	19
2.9.1	Offset of the Phase Center of the DUT from Center of Rotation	19
2.9.2	Offset of the Phase Center of the Calibrated Reference Antenna from Center of Rotation	20
2.9.3	Blocking Effect of the DUT on the Measurement Antenna (if too close)	20
2.9.4	Additional Measurement Uncertainties for Inadequate Measurement Distance	23
2.10	Signal Level Ripple Within Quiet Zone	24
2.10.1	Effect of Ripple on TRP and TIS Integration	24
2.10.2	Effect of Ripple on DUT Measurement for MIMO (Multiple Input Multiple Output)	28
2.10.3	Effect of Ripple on Range Reference Measurement	28
2.11	Quality of the Quiet Zone	29
2.11.1	Effect on DUT Measurement	29
2.11.2	Effect on Calibration Stage	29
2.12	Influence of the Ambient Temperature on the Test Equipment	29
2.13	Uncertainties Related to Testing with Near Field Phantoms	31
2.13.1	Estimation of Dielectric Parameter Measurement Uncertainties of Phantoms	31
2.13.2	Uncertainties Related to Testing with Head and Hand Phantoms	33
2.13.3	Uncertainties Related to Testing with Forearm Phantom Testing	46

2.13.4	Uncertainties Related to Testing with Chest Phantom (Informative) SISO, Anechoic.	53
2.13.5	Uncertainties Related to Testing with Ankle Phantom (Informative) SISO, Anechoic .	57
2.14	Positioning Misalignment	61
2.15	Misalignment of Positioning System	61
2.16	Positioning and Pointing Misalignment between the Reference Antenna and the Measurement Antenna	61
2.17	DUT Positioning/Repositioning Uncertainty	61
2.18	DUT Repositioning.....	62
2.19	Measurement Setup Repeatability	62
2.20	Receiver Performance Search Step Size	62
2.20.1	Fixed Step Size without Interpolation	62
2.20.2	Fixed Step Size with Interpolation	63
2.21	Grid Related Measurement Uncertainty	63
2.21.1	Coarse Sampling Grid for TIS Measurements below 6 GHz.....	63
2.21.2	Reduction in the Number of Test Samples on TIS Measurements below 6 GHz	63
2.21.3	Influence of Millimeter Wave TRP Measurement Grid	64
2.21.4	Influence of Millimeter Wave Spherical Coverage Grid.....	64
2.22	Miscellaneous Uncertainty.....	64
2.23	TIS Normalization Uncertainty.....	64
2.24	Linearization of RSS Measurements	65
2.25	Uncertainty of RSS Data from DUT	65
2.26	Reporting Mechanism for RSS Data from EU	66
2.27	Uncertainty Due to Difference in Gain Over Different Channel Bandwidths	66
2.28	Test System Frequency Flatness Uncertainty.....	66
2.29	Frequency Flatness for TIS Measurements	67
2.30	Uncertainty Due to Implementation of Mode-Stirring Sequence and Chamber Lack of Spatial Uniformity.....	68
2.31	Chamber Standing Wave	69
2.32	Standing Wave between Reference Calibration Antenna and Measurement Antenna	69
2.33	Phase Curvature.....	69
2.34	Influence of the XPD.....	69
2.35	Phase Center Offset of Calibration Antenna	74
2.36	Influence of the Calibration Antenna Feed Path.....	74
2.37	Influence of Noise	74
2.38	Systematic Error related to Beam Peak Search	74
2.39	Systematic Error Related to EIS Spherical Coverage	74
2.40	Minimum Measurement Distance Considerations	75
2.40.1	SISO, Anechoic Chamber Test Methodology.....	75
2.40.2	SISO, Millimeter Wave Test Methodology.....	75
2.41	Impact of ATF Pattern Error on TP.....	75
2.42	Impact of Non-Ideal Isolation between Streams in Radiated 2nd Stage.....	75

2.43	Multiple Measurement Antennas	75
Section 3	Assessment of Uncertainty Values using Simulation Tools (Normative)	76
3.1	Introduction	76
3.2	Requirements for the Simulation Software	76
3.3	Simulation Software Validation	76
3.4	Phone Validation.....	76
3.5	Computation of the Uncertainty for Type B Evaluation	77
3.6	Computation of the Uncertainty for Type A Evaluation	77
3.7	Numerical Evaluation of Head and Hand Phantom Fixtures Uncertainty.....	77
3.8	Numerical Evaluation of Device Positioning Uncertainty.....	77
3.9	Numerical Evaluation of Head, Hand and Forearm Phantom Shape Uncertainty	78
3.10	Numerical Evaluation of Head Phantom Support Material Uncertainty.....	78
Section 4	Lab Repeatability Evaluation (Normative)	79
Appendix A	Revision History.....	80

List of Figures

Figure 2.13.2.2-1 Ten Locations of Dielectric Measurements at the Brick Hand Surface	36
Figure 2.13.2.2-2 Ten Locations of Dielectric Measurements at the Fold Hand Surface	37
Figure 2.13.2.2-3 Ten Locations of Dielectric Measurements at the Narrow Data Hand Surface	37
Figure 2.13.2.2-5 Ten Locations for Dielectric Measurement of the Wide Grip Hand Surface	38
Figure 2.13.2.5.1-1 Phone Positioning Uncertainty Components	43
Figure 2.13.3.1-1 Coordinate System for Dielectric Test Locations	49
Figure 2.13.3.1-2 Twelve Locations for Dielectric Measurements on the Forearm Phantom	50
Figure 2.13.3.2-1 Forearm Positioning Uncertainty Components	52
Figure 2.13.4.1-1 Twelve Locations for Dielectric Measurements on the Chest Phantom	55
Figure 2.13.4.2-1 Chest Positioning Uncertainty Components	56
Figure 2.13.5.1-1 Twelve Locations for Dielectric Measurements on the Ankle Phantom	59
Figure 2.13.5.2-1 Ankle Positioning Uncertainty Components	60
Figure 2.34-1 Calibration Setup	69
Figure 2.34-2 Common Calibration approach based on Calibrating the Polarization Matched Signal Paths	70
Figure 2.34-3 Calibration Approach Based on Calibrating All Signal Paths	71
Figure 2.34-4 Signal Paths for Electric Fields (Based on Calibrating the Polarization Matched Signal Paths)	72

List of Tables

Table 1-2-1 Acronyms and Definitions	8
Table 2.9.4.1-1 Additional Measurement Uncertainties for Large Form Factor Devices	23
Table 2.13.1-1 Example of Uncertainty Template for Dielectric Constant (ϵ_r') or Conductivity (σ) Measurement at a Specific Frequency Band ¹	32
Table 2.13.2-1 Standard Uncertainties for the Head, Hand and DUT Positioning in the Hand and Against the Head	33
Table 2.13.2.6-1 Example of Uncertainty Assessment for Reasonably Worst-Case Head, Hand and DUT Positioning in the Hand and Against the Head	44
Table 2.13.2.7-1 Example of Uncertainty Assessment for Hand Phantom, Fixture and Phone Positioning in Data Mode Testing	46
Table 2.13.3-1 Standard Uncertainties for the Forearm, and DUT Positioning on the Forearm	46
Table 2.13.3.1-1 Coordinates of Ten Locations for Dielectric Measurements on the Forearm Phantom	48

Table 2.13.3.4-1 Example of Uncertainty Assessment for Reasonably Worst-Case Forearm and DUT Positioning on Forearm	52
Table 2.13.4.1-1 Coordinates of Twelve Locations for Dielectric Measurements on the Chest Phantom	54
Table 2.13.4.3-1 Example of Uncertainty Assessment for Reasonably Worst-case Chest and DUT Positioning on Chest.....	56
Table 2.13.5.1-1 Coordinates of Twelve Locations for Dielectric Measurements on the Ankle Phantom	58
Table 2.13.5.3-1 Example of Uncertainty Assessment for Reasonably Worst-case Ankle and DUT Positioning on Ankle	60
Table 2.34-1 XPD MU for Different XPD Values.....	71

Section 1 Introduction

1.1 Scope

This document provides more details on all measurement uncertainties associated with any of the OTA test methods in the CTIA OTA test plan.

1.2 Acronyms and Definition

Table 1-2-1 Acronyms and Definitions

Acronym/Term	Definition
Γ	Reflection Coefficient
3GPP	3 rd Generation Partnership Project
BER	Bit Error Rate
CAD	Computer-Aided Design
dB	Decibel
DFF	Direct Far-Field
DL	Downlink
DUT	Device Under Test
EIRP	Effective Isotropic Radiated Power
EIS	Effective Isotropic Sensitivity
EVM	Error Vector Magnitude
FER	Frame Error Rate
GNSS	Global Navigation Satellite System
IEEE	Institute of Electrical and Electronics Engineers
IFF	Indirect Far-Field
ISO	International Organization for Standardization
MU	Measurement Uncertainty
NIST	National Institute of Standards and Technology
NHPIS	Near-Horizon Partial Isotropic Sensitivity
NHPRP	Near-Horizon Partial Radiated Power
OCP	Open Circuit Potential
OTA	Over-the-Air
PCS	Personal Communications Service
PIGS	Partial Isotropic GNSS Sensitivity

Acronym/Term	Definition
PER	Packet Error Rate
RB	Resource Block
RF	Radio Frequency
PGRP	Partial GNSS Radiated Power
RSS	Receive Signal Strength or Root Sum of Square
RSAP	Reference Signal Antenna Power
RSARP	Reference Signal Antenna Relative Phase
RTS	Radiated Two Stage
S12, S21	Transmission Coefficient
SAM	Specific Anthropomorphic Mannequin
SAR	Specific Absorption Rate
SISO	Single Input Single Output
SNR	Signal to Noise Ratio
SSD	Surface Standard Deviation
TBD	To Be Determined
TIS	Total Isotropic Sensitivity
TRP	Total Radiated Power
UHS	Upper Hemisphere Isotropic Sensitivity
UHRP	Upper Hemisphere Radiated Power
VSWR	Voltage Standing Wave Ratio
XPD	Cross Polarization Discrimination

1.3 Document References

The following documents are referenced in this test plan:

Document Number, Document Name
[1] <i>Guide to the Expression of Uncertainty in Measurement published by the International Organization for Standardization (ISO) Geneva, Switzerland 1995.</i>
[2] CTIA 01.73, <i>Supporting Procedures</i>
[3] ETSI TR 102 273, <i>Electromagnetic compatibility and Radio spectrum Matters (ERM); Improvement on Radiated Methods of Measurement (using test site) and evaluation of the corresponding measurement uncertainties</i>
[4] CTIA 01.71, <i>Positioning Guidelines</i>
[5] CTIA 01.20, <i>Test Methodology, SISO, Anechoic Chamber</i>
[6] CTIA 01.40, <i>Test Methodology, MIMO, Multi-Probe Anechoic Chamber</i>
[7] CTIA 01.22, <i>Test Methodology, SISO, Millimeter Wave</i>
[8] ETSI TR 100 028, <i>Electromagnetic compatibility and Radio spectrum Matters (ERM); Uncertainties in the measurement of mobile radio equipment characteristics</i>
[9] NIS 81, <i>"The Treatment of Uncertainty in EMC Measurements,"</i> Ed. 1, NAMAS Executive, National Physical Laboratory, Teddington, Middlesex, TW11 0LW, England, 1994.
[10] <i>Dielectric Metrology with Coaxial Sensors</i>
[11] <i>The Uncertainties and Repeatability Limitations of Transmitter and Receiver Performance Assessments Posed by Head Phantoms</i>
[12] CTIA 01.72, <i>Near-Field Phantoms</i>
[13] IEEE 1528-2002
[14] NIST, <i>Guidelines for evaluating and expressing the uncertainty of NIST measurement results</i> , Technical Note 1297 (TN 1297), United States Department of Commerce Technology Administration, National Institute of Standards and Technology, Gaithersburg, MD, 1994.
[15] CTIA 01.90, <i>Informative Reference Material</i>
[16] CTIA 01.21, <i>Test Methodology, SISO, Reverberation Chamber</i>
[17] CTIA 01.03, <i>Reporting Tables</i>
[18] IEEE P1528.1™/D1.0 Draft Recommended Practice for Determining the Peak Spatial-Average Specific Absorption Rate (SAR) in the Human Body from Wireless Communications Devices, 30 MHz - 6 GHz: General Requirements for using the Finite Difference Time Domain (FDTD) Method for SAR Calculations
[19] IEEE P1528.4™/D1.0 Draft Recommended Practice for Determining the Peak Spatial Average Specific Absorption Rate (SAR) in the Human Body from Wireless Communications Devices, 30 MHz - 6 GHz: Requirements for Using the Finite-Element Method for SAR Calculations, specifically involving Vehicle-Mounted Antennas and Personal Wireless Devices

Document Number, Document Name

- [20] IEEE P1528.3™/D2.0 Draft Recommended Practice for Determining the Peak Spatial-Average Specific Absorption Rate (SAR) in the Human Body from Wireless Communications Devices, 30 MHz - 6 GHz: General Requirements for using the Finite Difference Time Domain (FDTD) Modeling of Mobile Phones/Personal Wireless Devices

Section 2 Treatment of Measurement Uncertainty Components

The chosen method for calculation of the measurement uncertainty is based on the *Guide to the Expression of Uncertainty in Measurement* [1].

The ISO guide gives a general approach to calculating measurement uncertainty that is applicable to all types of measurements. The process involves the combination of the standard deviations (generally known as standard uncertainties) of the individual contributors by the root-sum-of-squares method. This method assumes that all systematic errors have been identified and, to the greatest extent possible, corrected for. Remaining individual components of uncertainty are assumed to be random in nature such that they can be combined as normal distributions. Note that this may not be the case when combining multiple identical measurements in series. Likewise, multiple parallel measurements (e.g., the different paths in the test system) do not reduce the systematic error contribution through averaging.

Using the above approach, the following illustrates the practical steps involved:

1. Compile a complete list of the individual components of measurement uncertainty that contribute to a measurement;
2. Determine the maximum value of each component of uncertainty;
3. Determine the distribution of each component of uncertainty (rectangular, U-shaped, etc.);
4. Calculate (if necessary) the standard uncertainty, u_i , of each component of uncertainty;
5. Convert the units (if necessary) of each component of uncertainty into the chosen unit, i.e. dB;
6. Combine the standard uncertainties by the root-sum-of-squares method to derive the total combined standard uncertainty, $u_{c\text{total}}$;
7. Under the assumption that the probability distribution of the combined standard uncertainty is Gaussian/Normal, multiply the resulting combined standard uncertainty by an expansion factor ' k ' (taken from Student's T-distribution, W.S. Gosset 1908) to derive the 'expanded uncertainty,' U_e , for a given confidence level. All expanded uncertainties are quoted to 95% confidence level, so k is taken as 2 (theoretically k should be 1.96, but for convenience, the value 2 had been agreed upon). Expressed a different way, this gives 95% confidence that the true value is within 2 times the combined standard uncertainty of the measured value:

Equation 2-1

$$U_e = 2 \cdot u_{c\text{total}} = 2 \cdot \sqrt{\sum u_i^2}$$

The individual components of uncertainty are combined separately to find the combined uncertainty related to the DUT and reference measurements. These are then combined and expanded as:

Equation 2-2

$$U_e = 2 \cdot \sqrt{u_{\text{contribution of the DUT measurement}}^2 + u_{\text{contribution of the reference measurement}}^2}$$

The value for each component of uncertainty is determined as discussed in the following sections. Relative uncertainty parameters can also be determined by simulations provided that it can be guaranteed that the relative accuracy is significantly better than 0.1 dB (see Section 3).

Note that certain test plans may include systematic uncertainties that are not corrected for. These are added directly to the total combined standard uncertainty to derive the total expanded uncertainty as described in the specific test plan

2.1 Mismatch

This uncertainty contribution addresses variation in the test system VSWR that introduces measurement uncertainty. For automated test systems used for OTA testing, it is expected that there will be impedance mismatch between the various RF cables and components used within the system. Standing waves occur in cables between points of mismatch and can cause variations in the measured signal levels. At the frequencies of interest, longer cables tend to be self-attenuating, resulting in a reduction in the standing wave contribution. In other cases, attenuators may be added at connection ports to reduce standing wave effects. The assumption made here is that any standing wave contributions in the cable only serve to modify the resultant signal level, but do not introduce sufficient time delay to corrupt the digital communication being measured. In this case, the error in a measurement due to mismatches throughout the system is caused by the difference in the VSWR between the calibration step (where the path loss of cables and other components of the measurement system is determined) and the measurement step (where those cables and components are used in a power or sensitivity measurement). If only the magnitude of the mismatch at a given connection were to change, then the measurement uncertainty for that change could be estimated using the difference in VSWR magnitudes before and after the change. However, more often, the change in the system also entails a change in cable lengths between two mismatches. That change in cable length results in a change in the frequency dependence of the mismatch, which makes it impractical to try to consider the difference between VSWR values to determine the uncertainty. Instead, the VSWR uncertainty due to each mismatch where a cable connection is changed must be applied to determine the appropriate measurement uncertainty contributions.

The maximum error due to VSWR between two ports is given in general form by the following equation:

Equation 2.1-1

$$\varepsilon_{VSWR} = 20\log(1 + |\Gamma_1| \times |\Gamma_2| \times |S_{21}| \times |S_{12}|)$$

Where Γ_1 and Γ_2 are the complex reflection coefficients of the two ports in question and S_{21} and S_{12} are the forward and reverse transmission coefficients between the two ports. From this it is evident that reducing the reflection coefficients (by reducing mismatches) or reducing the transmission coefficients (by adding attenuation) will reduce the resulting error contribution. The reflection coefficient can be expressed in terms of the VSWR at a given connector by [Equation 2.1-2](#).

Equation 2.1-2

$$|\Gamma| = \frac{VSWR - 1}{VSWR + 1}$$

From this equation, a simpler two-port formulation can be derived to represent the VSWR error contribution due to the reflectivity of each side of a cable connection point. This allows estimating the required uncertainty contribution by simply measuring the reflection coefficients of each side of a cable connection that is changed between the calibration and measurement steps.

Equation 2.1-3

$$\begin{aligned}\varepsilon_{VSWR} &= 20\log(1 + |\Gamma_1| \times (|\Gamma_2| \times |S_{21}| \times |S_{12}|)) \\ &= 20\log(1 + |\Gamma_{source}| \times |\Gamma_{load}|)\end{aligned}$$

where Γ_{source} and Γ_{load} are the complex reflection coefficients of the cable/connector ends looking towards the source or load respectively.

For example, in the calibration procedure in Section 4.4 of *CTIA 01.73* [2], there are four principal mismatch contributions that come from: 1) the loopback cable connection made to calibrate out cable losses and test equipment factors during the range calibration; 2) the connection between the “transmit” cable and the reference antenna placed within the quiet zone; 3) the connection between the measurement port cable of the test system (the cable normally connected to the test equipment to route signals to or from the measurement antenna) and the loopback cable; and 4) the connection of the measurement port cable to the test equipment. The impact of the first three contributions can be minimized through the use of appropriate attenuators at the end of the transmit and loopback cables. The fourth term can be reduced through the addition of an attenuator that remains in the measurement system on the end of the cable leading to the measurement instrument.

Since the error due to VSWR has a sinusoidal nature, it causes a deviation that clusters equally above and below the initial transmitted signal. This U-shaped distribution must be converted to an equivalent normal distribution probability by using the following equation to determine the standard uncertainty.

Equation 2.1-4

$$u_i = \frac{a_1}{\sqrt{2}} = \frac{\varepsilon_{VSWR}}{\sqrt{2}}$$

2.1.1 Special Requirement for SISO, Millimeter Wave

For Millimeter-Wave Wireless Device OTA Performance testing, special care must be taken for the environmental conditions (temperature, humidity, etc.) to remain stable over time to ensure that the phase and amplitude of the standing waves between the various system components remain the same between the system calibration and device measurements.

2.2 Cable Factor

This uncertainty applies to the Measurement Antenna only.

For cases in which the Measurement Antenna is directional (i.e. peak gain greater than +5 dBi e.g. horn etc.), the standard uncertainty should be taken as 0.00 dB. For all other cases of Measurement Antenna gain (i.e. dipole, sleeve dipole, loop, etc.), the following rules apply:

- If nothing has been changed in the time interval between the Range Reference Measurement and the DUT measurement, the interaction of the cable (whether it is 'dressed' in ferrites and/or a balun) will be the same in both parts of the test, so a fixed value of 0.00 dB shall be taken for the expanded uncertainty contribution.
- If the cable has been changed or moved to a different routing, but the dressing with ferrites and/or a balun remains the same (or similar), then a fixed value of 0.50 dB shall be taken and its distribution shall be assumed to be rectangular (i.e. standard uncertainty = 0.29 dB).
- If the dressing has been changed and ferrites and/or balun have only been present in one of the parts of the test, then 0.00 dB shall be entered in the measurement part of the test, and 4.00 dB in the Range Reference Measurement (justification for these values can be found in Annex A, section A.5 and Annex E in TR 102 273 [3]).

2.3 Insertion Loss

Where the same cable on the input to the Measurement Antenna has been used in both parts of the test, then a fixed value of 0.00 dB shall be entered into the tables for both parts of the test.

Where any cable or other system component is used in only one part of the test (e.g. as part of an external cable loop for the Range Reference Measurement) and its insertion loss is used in the calculations, then either the overall combined standard uncertainty of the insertion loss measurement shall be used in the relevant table or the manufacturer's data sheet shall be consulted. In the latter case, this uncertainty will usually be quoted as $\pm x$ dB. Unless something specific is stated about the distribution of this uncertainty, it should be assumed to be rectangularly distributed, in which case the standard uncertainty shall be calculated as:

$$\frac{\text{maximum value}}{\sqrt{3}}$$

2.4 Receiving Device

The receiving device, such as spectrum analyzer, base station simulator) is used to measure the received signal level either as an absolute level or as a relative level. It generally contributes to the uncertainty components in two ways: absolute level accuracy and non-linearity. The components which impact the uncertainty of the measurement depend on the measurement procedure.

For TRP and EIRP measurements, both absolute level accuracy and non-linearity components apply.

For individual absolute power measurements, if the manufacturer's datasheet provides the absolute level uncertainty specification that encompasses all contributions, this specification is usually all that is needed. In some cases, manufacturer's data sheets may not provide a single absolute uncertainty specification and may require combining multiple specifications to obtain the correct value u .

For relative measurements such as range calibration and single-point offset measurements, if the same receiver is used to measure both test configurations, then the receiving device is used to measure the relative received signal levels. The receiving device can generally contribute uncertainty components in terms of non-linearity for this measurement. If two different instruments are used (including, possibly, two different options in the same base station simulator) then the absolute uncertainties of both devices will contribute and shall be included.

These uncertainty contributions shall be taken from the manufacturer's data sheet and converted to dB if necessary. The worst case data sheet values shall be used.

Note that the measurement uncertainty specification of the instrument may vary as a function of the chosen bandwidth setting or other parameters. The lab shall ensure that appropriate manufacturer's uncertainty contributions are specified for the settings used.

2.5 Signal Generator or Base Station Simulator

In a similar manner to the receiving device, the signal generator or base station simulator can contribute in two ways, absolute level and stability. The uncertainty terms that need to be considered depend on the measurement process.

For individual absolute power measurements such as the receiver sensitivity test, if the manufacturer's datasheet provides the absolute level uncertainty specification that encompasses all contributions, this specification is usually all that is needed. In some cases, manufacturer's data sheets may not provide a single absolute uncertainty specification and may require combining multiple specifications to obtain the correct value.

For relative measurements, if the same base station simulator is used to measure both test configurations, then it is used to measure the relative radiated sensitivity. In this case, the base station simulator will generally contribute uncertainty components in terms of non-linearity for the relative measurement. If two different instruments are used (including, possibly, two different options in

the same base station simulator) then the absolute uncertainties of both devices will contribute. In that case the absolute uncertainty of the base station simulator for test configuration B would be included as an additional uncertainty.

In the case of a network analyzer, the signal generator is combined with the receiver in one unit that measures the relative difference between the output signal and received signal. Thus, the uncertainty contribution of the signal generator is included in one overall uncertainty contribution of the instrument and does not need to be entered separately.

These uncertainty contributions shall be taken from the manufacturer's data sheet and converted to dB if necessary.

1. If using the manufacturer's data sheet, the worst-case values shall be used.
2. An allowed alternative is to use an alternate measurement device to normalize the signal generator RF output level.
3. An allowed alternative is to use the calibration report plus the MU and aging terms from the calibration lab.

For certain test configurations, the confidence level for BER/FER for measuring the sensitivity may be limited in order to keep the test time low. The measured sensitivity with lower confidence levels will have some small variation. For the full TIS measurements, the variation for each sensitivity reading will largely average out over the large number of sample points over the 3D sphere. However, for a single point measurement, this small variation in sensitivity shall be included as an uncertainty. One way to mitigate this uncertainty is to use a much higher confidence level (i.e. longer test time) to significantly reduce this uncertainty. For the multi-point measurement, the small variation in radiated sensitivity is averaged over multiple points and its uncertainty is reduced by the averaging process. Test measurements can be conducted to characterize the uncertainty associated with whichever test method (such as using a higher confidence level) is selected for the single/multi point radiated measurement.

2.6 Network Analyzer

This contribution originates from all uncertainties involved in transmission magnitude measurement with a network analyzer, e.g., drift, frequency flatness, temperature variation from kit calibration to path losses measurement as well as interpolation of calibration data if test frequencies were not calibrated during path loss characterization. The uncertainty value will be indicated in the manufacturer's data sheet. It needs to be ensured that appropriate manufacturer's uncertainty contribution is specified for the settings (IF bandwidth, power levels, etc.) used.

When an end-to-end system calibration approach is used, the absolute levels are related to the total system losses of the measurement path. When a split calibration approach is used, separate MU contributions need to be determined.

- u_{cond} : transmission magnitude uncertainty for the conducted portion of the calibration; the absolute levels are related to the total system losses for the portion of the system calibrated
- u_{rad} : transmission magnitude uncertainty for the radiated portion of the calibration; the absolute levels are related to the total system losses for the portion of the system calibrated

The total MU of the network analyzer for the split calibration is the RSS'ed value of u_{cond} and u_{rad} .

2.7 Amplifier

The uncertainty associated with the external amplifier is contingent on the system setup and calibration method.

2.7.1 Gain

If the external amplifier has been characterized individually then the measurement uncertainty associated with the gain measurement should be included in the overall uncertainty. If the external amplifier has been characterized as part of the system, then there is no additional uncertainty over that of the associated system path loss measurement.

2.7.2 Mismatch

If the external amplifier has been characterized individually then the mismatch uncertainty at both the input and output should be included in the overall uncertainty. If the external amplifier is used for both measurement and calibration stages, the uncertainty contribution associated with it can be considered systematic and constant: 0 (zero).

For more information on the mismatch uncertainty see Section [2.1](#).

2.7.3 Stability

This term quantifies the stability of the output signal over time. This term needs to be considered for all systems in which an external amplifier is present. Even if the amplifier is part of the system for both measurement and calibration, the uncertainty due to the stability shall be considered. The stability shall be evaluated for the range of laboratory conditions seen during normal operation, including any variation in initial conditions and laboratory temperature. The variation may be measured directly over a minimum of 24 hours of normal operating conditions (e.g., three non-contiguous eight hour-sessions) or determined from manufacturer's specifications if the stability as a function of laboratory conditions are clearly indicated.

2.7.4 Linearity

The linearity of the amplifier comes into play when the system or amplifier calibration is performed at a different input/output level than will be used during the DUT test. This uncertainty can be either measured or determined by the manufacturers' data sheet.

2.7.5 Amplifier Noise Figure/Noise Floor

All amplifiers add noise to the signal that they amplify, reducing the SNR at the output compared to that at the input. As the signal level input to the amplifier is lowered, the resulting signal + noise may be measurably higher than the signal alone. More importantly for a receiver sensitivity test, the noise of the amplifier plus the amplified noise of the signal source could become significant relative to the platform noise. Thus, the noise floor of the amplifier defines an absolute minimum of the linear dynamic range of the system. The error introduced in the desired signal affects the EVM of the signal and correspondingly the chances of the receiver to decode the signal. This can be treated as a voltage error due to the noise power:

Equation 2.7.5-1

$$\varepsilon_{EVM} = 20 \cdot \log \left(1 + 10^{\frac{-SNR}{20}} \right)$$

where SNR is the signal to noise ratio in dB at the signal level used for the SIR_test.

The noise power can be assumed to be Gaussian and thus simply summed with the interference power. The error in the interference power due to the noise is thus:

Equation 2.7.5-2

$$\varepsilon_{INR} = 10 \cdot \log \left(1 + 10^{\frac{-INR}{10}} \right)$$

where INR is the interference to noise ratio in dB.

2.8 Reference Antenna

2.8.1 Gain Reference

The calibrated reference antenna only appears in the reference measurement where the gain uncertainty has to be taken into account. This uncertainty shall come from a calibration report with traceability to a National Metrology Institute with measurement uncertainty budgets generated following the guidelines outlined in internationally accepted standards.

For cases in which the Calibrated Reference Antenna is directional (i.e., peak gain greater than +5 dBi e.g., horn etc.), the standard uncertainty shall come from its calibration report.

For all other gain based reference measurements (i.e., dipole, sleeve dipole, loop, etc.), the following rules apply:

- Where the gain of the calibrated reference antenna has been measured in a different test chamber using the same mounting arrangements/jigs, the value of the gain standard uncertainty shall be taken as the reported value from that measurement.
- Where the gain of the calibrated reference antenna has been measured in a different test chamber using different mounting arrangements/jigs, the value of the standard gain uncertainty shall be taken as the reported value from that measurement, combined by the RSS method with a contribution from the mounting arrangement/jig. A fixed value of 0.5 dB shall be taken and its distribution shall be assumed to be rectangular (i.e. standard uncertainty = 0.29 dB).
- Where the gain of the calibrated reference antenna has been measured in the same test chamber (possibly by the 3-antenna method for gain) using the same mounting arrangements/jigs, the value of the standard gain uncertainty shall be taken as that calculated for the measurement.

2.8.2 Efficiency Reference

The measured average transmission level in the reference measurement is directly related to the stated radiation efficiency of the calibrated reference antenna. Therefore, the uncertainty of the radiation efficiency value is directly transferred to the uncertainty calculation of the reference measurement.

This component of uncertainty shall be taken as the uncertainty stated by the laboratory that calibrates the reference antenna.

2.8.3 Unknown K factor

This component accounts for differences in the radiation pattern of the reference and DUT antennas that can lead to differences in the reference power transfer function in loaded chambers. Specifically, when an IoT device is measured with a phantom, the difference in the radiation patterns of the two antennas (reference and DUT + phantom) may be significant due to blockage by the phantom. Currently, 0.35 dB is considered a worst-case bound. Labs are expected to incur less than 0.35 dB uncertainty in their reference measurement due to this effect.

This effect can be represented as an asymmetric uncertainty contribution of + worst-case bound / - 0 dB, with a rectangular distribution. The asymmetric uncertainty can be converted to a symmetrical uncertainty by applying an offset to the corresponding measurement value and dividing the total range of the expanded uncertainty by two. Using the procedure discussed in Section 2.20.1, for the purposes of this test plan, this uncertainty contribution is assumed to be symmetrical about the estimated G_{ref} result. Thus, a fixed uncertainty contribution of ± 0.175 dB with a rectangular distribution (standard uncertainty contribution of 0.101 dB) should be reported for the Unknown K Factor uncertainty.

2.9 Measurement Distance

2.9.1 Offset of the Phase Center of the DUT from Center of Rotation

2.9.1.1 Head Phantom

All head phantom measurements defined in this test plan require θ and ϕ rotation of the DUT and head phantom combination about the Ear Reference Point (assumed to be the location of the phase center) as the coordinate origin. As this may be practically impossible for a number of reasons (e.g. the turntable may be too small to allow adequate offset, etc.), an alternative of rotating about the center of the SAM head phantom is allowed. The center of the SAM head phantom is defined as the new origin of the coordinate system if the axes are translated 82 mm in the -Y direction from the original origin shown in CTIA 01.71 [4]. The new alignment is shown in CTIA 01.71 [4]. For this new alignment, an additional uncertainty contribution must be included in the calculation of measurement uncertainty for the DUT measurement because the phase center will rotate on a non-zero radius about the center of rotation, thereby giving a variable measurement distance.

The maximum level change due to this alternative positioning of the SAM head is:

$$20\log_{10}\left(\frac{d}{d - 0.082}\right) \text{ dB}$$

where d = range length i.e. the distance between the phase center of the measurement antenna and the axis of rotation of the turntable (ϕ -axis for distributed-axes positioner systems, θ -axis for combined-axes positioner systems).

Note: “ d ” is in meters.

Since this level change uncertainty is assumed to be rectangularly distributed, the standard uncertainty shall be derived by dividing the maximum level by $\sqrt{3}$.

2.9.1.2 Notebook Computer

In many cases the location of an embedded antenna in a notebook computer will be unknown by the lab performing the tests. Hence it will be impossible to place the phase center of the DUT on the axis of rotation. The antenna radiation patterns will be affected by the change in free space dispersion as the phase center moves towards and away from the measurement antenna. The maximum effect of this phenomena is given by:

$$\Delta = 20\log_{10}\left(\frac{d + 1}{d - 1}\right) \text{ dB}$$

where d is the range length and l is one half of the largest single dimension of the DUT and Δ is the maximum change in the pattern level due to effect. For a range length of 120 cm and a notebook computer with a single largest dimension of 42 cm, this results in a change in received signal level of 3.07dB. However, when the individual measurement points are integrated into a value for TRP or TIS, this effect is greatly reduced. For every point on the front of the measurement sphere where the measured signal level is higher than it should be, there is a corresponding point on the rear of the measurement sphere where the signal level is lower than it should be.

The uncertainty contribution for this effect is included in the uncertainty contribution for measurement distance given in Section 2.9.4.1 and no additional uncertainty contribution is required.

2.9.2 Offset of the Phase Center of the Calibrated Reference Antenna from Center of Rotation

For the Range Reference Measurement (i.e, where the Calibrated Reference Antenna is involved), any uncertainty in the accuracy of positioning its phase center on the axis(es) of rotation will directly generate an uncertainty in this part of the measurement. For sleeve dipoles and loops, provided that care is taken in their positioning the uncertainty should be 0.00 dB since their phase centers are easily identifiable.

However, for ridged horn antennas (for which the position of the phase center varies with frequency), the phase center could be at any point within the tapered sections, giving:

- For a ridged horn: A maximum positional uncertainty, $\pm d$, where d equals 0.5 times the length of taper.

The level uncertainty resulting from these positional uncertainties shall be calculated as:

Equation 2.9.2-1

$$\pm 20 \log_{10} \left(\frac{\text{measurement distance} - d}{\text{measurement distance}} \right)$$

Since this level uncertainty is assumed to be rectangularly distributed, the standard uncertainty shall be derived by dividing by $\sqrt{3}$.

2.9.3 Blocking Effect of the DUT on the Measurement Antenna (if too close)

This uncertainty arises because the DUT can 'block' the power radiated by the Measurement Antenna, reflecting the energy back into the antenna which, as a result, can change its input impedance/VSWR whilst also creating a standing wave within the chamber between the Measurement Antenna and DUT. The magnitudes of the resulting uncertainties are dependent on both the directionality of the Measurement Antenna and the measurement distance. The uncertainties increase with increasing directionality (i.e., increasing gain) of the Measurement Antenna and with decreasing measurement distance. The magnitudes of the effects will vary as the DUT and/or Measurement Antenna is rotated (since the 'blocking' area changes with angle), and therefore allowances for the uncertainties introduced shall be made.

Note: *These uncertainties only apply for tests of the DUT against the head phantom or for notebooks and other large form factor devices. The contributions can be expected to be worst for large flat reflecting objects such as a notebook display or large metallic housings. These terms may also apply to the range calibration in the event that the reference antenna has a large radar cross section. Note too that significant changes in VSWR at range lengths on the order of a few wavelengths from the reference channel may be indicative of the reference channel encroaching on the reactive region of the measurement antenna, thus invalidating measurement results.*

2.9.3.1 VSWR

This contribution covers the potential free-space standing wave between the measurement antenna and any large DUT within the test volume. As described in Section 2.1, measurement uncertainty arises when the VSWR changes between the range calibration and DUT measurement.

Devices such as notebooks present large flat surfaces to the measurement antenna. There is the possibility that a large amount of energy incident to the DUT will be reflected back to the measurement antenna.

To estimate the magnitude of this uncertainty, Equation 2.9.3-1 is used to evaluate the potential standing wave contribution from reflections within the test volume to the first notable mismatch past the measurement antenna.

Equation 2.9.3-1

$$\begin{aligned}\varepsilon_{VSWR} &= 20\log\left(1 + |\Gamma_{DUT}| \times \frac{G_{MA}\lambda}{8\pi R} \times (|\Gamma_2| \times |S_{21}| \times |S_{12}|)\right) \\ &= 20\log\left(1 + |\Gamma_{DUT}| \times \frac{G_{MA}\lambda}{8\pi R} \times |\Gamma_{load}|\right)\end{aligned}$$

Where $G_{MA}\lambda/8\pi R$ is a modified version of the Friis transmission equation representing the measurement antenna (MA) with linear power gain G_{MA} both transmitting and receiving the signal reflected from the DUT at a distance R from the MA, for a total distance of $2R$. Since the gain of the measurement antenna includes the effect of mismatch on the antenna, there is no need to further evaluate the VSWR of the measurement antenna itself. The S-Parameters in Γ_{load} correspond to the path loss of any cables and attenuators between the measurement antenna and the first significant mismatch Γ_2 . As described in Section 2.1, this can be replaced by a single measurement of the mismatch at the end of the cable attached to the measurement antenna. To determine the worst-case possible error contribution due to this term, Γ_{DUT} may be set to 1 to represent a perfectly reflecting metal plane normal to the measurement antenna boresight. The maximum error due to this term is then converted to a standard uncertainty contribution as described in Section 2.1.

Example:

Range length: 1.2 m

Measurement antenna gain: 9 dB

Test frequency: 700 MHz

Cable loss: 3 dB

Mismatch at test equipment rack: 2:1

Equation 2.9.3.1-1

$$\begin{aligned}\epsilon_{VSWR} &= 20\log\left(1 + \frac{10^{9/10} \times \frac{c}{7 \times 10^8}}{8\pi \times 1.2} \times \left(\frac{2-1}{2+1} \times 10^{-3/20} \times 10^{-3/20}\right)\right) \\ &= 20\log\left(1 + \frac{7.94 \times 0.428}{8\pi \times 1.2} \times \left(\frac{1}{3} \times 0.707^2\right)\right) \\ &= 0.16 \text{ dB}\end{aligned}$$

Note: Any significant change in the VSWR of the measurement antenna would imply a reactive region interaction, implying that the measurement antenna is too close to the DUT and thus the test system should not be used in this case.

2.9.3.2 Chamber Standing Wave

In addition to the second order VSWR term described above, there is the potential for a standing wave reflection between the measurement antenna and the DUT, representing an additional chamber ripple term beyond that recorded in the ripple test. While this contribution may tend to average out over the surface of an irregular object, that cannot be guaranteed. This term is also a function of the reflectivity of the measurement antenna, which may be difficult to determine empirically. If a measured or manufacturer specified reflectivity is unavailable, then for the purpose of this contribution, the reflectivity of the measurement antenna shall be assumed to be the gain of the measurement antenna multiplied by the reflectivity corresponding to the VSWR of the MA. Thus, [Equation 2.9.3.1-1](#) above becomes:

Equation 2.9.3.2-1

$$\epsilon_{VSWR} = 20\log\left(1 + |\Gamma_{EUT}| \times \frac{G_{MA}\lambda}{8\pi R} \times |\Gamma_{MA,VSWR}|\right)$$

Given the same example parameters above, and a measurement antenna VSWR of 2.5:1, this contribution then becomes:

Equation 2.9.3.2-2

$$\begin{aligned}\epsilon_{VSWR} &= 20\log\left(1 + \frac{10^{9/10} \times \frac{c}{7 \times 10^8}}{8\pi \times 1.2} \times \frac{2.5-1}{2.5+1}\right) \\ &= 20\log\left(1 + \frac{7.94 \times 0.428}{8\pi \times 1.2} \times .429\right) \\ &= 0.41 \text{ dB}\end{aligned}$$

If a free-space reflectivity of the measurement antenna is available, [Equation 2.9.3.2-2](#) simplifies to:

$$\varepsilon_{V_{SWR}} = 20 \log \left(1 + |\Gamma_{EUT}| \times \frac{\lambda}{8\pi R} \times |\Gamma_{MA}| \right)$$

2.9.3.2.1 Special Considerations for Notebook Computers

For notebook computers, these standing waves contribute to measurement uncertainty in much the same way as reflections from the chamber surfaces and positioning equipment. However, measurements have shown that even with a notebook computer and a short measurement distance, this effect causes a change in measured TRP of less than 0.1 dB. As a result, no additional uncertainty contribution is required.

2.9.4 Additional Measurement Uncertainties for Inadequate Measurement Distance

The minimum measurement distances given in Table 2-1 in *CTIA 01.73 [2]* are based on industry accepted “rules of thumb” for single point measurements. Small (< 30 cm) form factor devices shall meet the minimum measurement distances given in Table 2-1 of *CTIA 01.73 [2]*. Reducing the minimum measurement distance while taking an additional MU for inadequate measurement distance is for further study.

2.9.4.1 Special Considerations for Notebook Computers

When measuring DUTs with a dimension exceeding 30 cm, there is an additional uncertainty term related to measurement distance which must be included.

Only notebooks whose single largest dimension is less than or equal to 42 cm shall be tested. Range lengths equal to or greater than the minimum range lengths specified in *CTIA 01.73 [2]* of the test plan shall be used.

If the single largest dimension of the notebook computer under test exceeds 30 cm, an additional measurement uncertainty contribution must be included in the measurement uncertainty budget. The additional contribution is shown in [Table 2.9.4.1-1](#) below. The values for the additional uncertainty contributions were determined from numerical simulations assuming the worst-case scenario of a large notebook with the antenna located in the top corner of the screen.

Table 2.9.4.1-1 Additional Measurement Uncertainties for Large Form Factor Devices

Frequency Range	Additional Uncertainty Contribution Required
617-1186.68 MHz	0.25 dB
1574-2360 MHz	0.20 dB
2496-5925 MHz	No impact on integrated measurements.

Note: The rationale for the additional uncertainty contributions of [Table 2.9.4.1-1](#) is the following: The minimum range for large (> 42 cm) device is larger than that for small (< 30 cm) devices. The MU contribution is based on worst-case simulations, only small impact on integrated measurements is foreseen.

Note: Please refer to *CTIA 01.73 [2]* for derivation of Measurement Distance lower bound.

2.9.4.2 Special Considerations for Multiple Antennas Radiating Coherently

In cases where multiple antennas integrated in the DUT radiate coherently and have an effective radiating aperture greater than what is assumed in this test plan, no additional measurement uncertainty shall be assessed. See Section 2 of *CTIA 01.73* [2] for more details.

2.10 Signal Level Ripple Within Quiet Zone

The signal level ripple is measured during the chamber proving procedures detailed in *CTIA 01.73* [1] using omni-directional probe antennas (sleeve dipoles and loops). The ripple test provides a very thorough measurement of the interaction of the chamber and positioning equipment with different signal paths throughout the quiet zone. The ripple test result represents a worst-case deviation in EIRP or EIS for a theoretical isotropic radiator/receiver or an omni-directional radiator/receiver with the same orientation as the ripple test.

For notebooks whose single largest dimension exceeds 30 cm, the ripple test measurements shall be repeated using a similar process as for smaller devices except that offsets shall be used as described in Section 5.4 of *CTIA 01.73* [2] to ensure that the quiet zone has been characterized for the test volume of the DUT.

Suitable values for the measurement uncertainties associated with different measurement quantities can be determined as described in Section 2.10.1.

2.10.1 Effect of Ripple on TRP and TIS Integration

In TRP and TIS tests, the test metric (quantity used for comparison between DUTs) is the result of a spherical surface integral of the EIRP or EIS. In order to estimate the effect of a single EIRP/EIS point on the total integrated value, it is necessary to define a statistical uncertainty value referred to as the surface standard deviation (SSD). The SSD uses the ripple test results to determine a Type A uncertainty value for a theoretical isotropic radiator placed anywhere within the quiet zone. Empirical results of both measured and calculated omni-directional and directional antennas indicate that the uncertainty predicted by the SSD of the ripple encompasses the variation in the TRP/TIS integral value for the expected range of DUT patterns.

The standard deviation from a sample of N readings is given by:

Equation 2.10.1-1

$$s(q_k) = \sqrt{\frac{1}{(N-1)} \sum_{k=0}^{N-1} (q_k - \bar{q})^2}$$

In terms of relative deviations in linear power, this becomes:

Equation 2.10.1-2

$$s(p_k) = \sqrt{\frac{1}{(N-1)} \sum_{k=0}^{N-1} \left(\frac{p_k}{\bar{p}} - 1\right)^2}$$

where p_k is an individual ripple measurement point, converted to linear units

$(p_k = 10^{p_{k(dB)/10}})$ and \bar{p} is the average of the associated ripple measurement, again in linear units. This formulation provides the SSD for the phi-axis ripple test, since the contribution of the EIRP/EIS to the surface integral is the same at each phi angle.

For the theta-axis ripple, the contribution of each EIRP/EIS point to the surface integral is dependent on the theta angle, and therefore, so does any error contribution due to that point. The spherically weighted contribution becomes:

Equation 2.10.1-3

$$s(p_k) = \sqrt{\frac{1}{N-1} \sum_{k=0}^{N-1} \left[\left(\frac{p_k}{\bar{p}} - 1 \right) \sin(\theta_k) \right]^2}$$

Note: This simplifies to the previous equation when $\theta = 90^\circ$.

The standard uncertainty contribution due to the ripple test is then given by the maximum of all the $s(p_k)$ values for all orientations, offsets, and polarizations of the ripple test:

Equation 2.10.1-4

$$u(x) = 10 \log \left(1 + \max(s_j(p_k)) \right)$$

Equation 2.10.1-4 represents the value to be placed in the table in *CTIA 01.73* [2] for $N > 50$. For $N \leq 50$, an appropriate coverage factor should be applied.

2.10.1.1 Applying the Surface Standard Deviation

Repeat the following steps for each required band and positioning system configuration (free-space vs. SAM head phantom, etc.) to generate the uncertainty for that configuration.

For each ripple test measurement:

- Compute the linear average of the ripple value.
- Calculate the spherically weighted surface standard deviation using Equation 2.10.1-3. Use $\theta = 90^\circ$ for phi-axis ripple test results.
- Select the maximum SSD from all 13 ripple test positions and calculate the standard uncertainty in dB using Equation 2.10.1-4. This value shall be used directly in the uncertainty budget in the table in *CTIA 01.20* [5].

2.10.1.2 Analysis of Uncertainty vs. Error Contribution

In order to provide some confidence in the uncertainty values produced by this method, it is useful to compare the actual error contribution to a TRP/TIS integral to the uncertainty predicted by a ripple test. This can only be performed rigorously by assuming an isotropic radiation pattern for the DUT, but as mentioned above, the result is deemed reliable for other non-isotropic DUTs of interest to this test plan. It is easy enough to test specific cases and show that the SSD expanded uncertainty encompasses the TRP/TIS error for likely real pattern shapes. This formulation will refer solely to TRP, but the same procedure can be followed for TIS.

Starting with the following equation for TRP:

Equation 2.10.1.2-1

$$TRP \cong \frac{\pi}{2NM} \sum_{i=1}^{N-1} \sum_{j=0}^{M-1} [EiRP_{\theta}(\theta_i \phi_j) + EiRP_{\phi}(\theta_i \phi_j)] \sin(\theta_i)$$

In terms of total EIRP and an associated error term at each point, this becomes:

Equation 2.10.1.2-2

$$TRP + Error_{TRP} \cong \frac{\pi}{2NM} \sum_{i=1}^{N-1} \sum_{j=0}^{M-1} [EiRP_{Total}(\theta_i, \phi_j) + Error(\theta_i, \phi_j)] \sin \theta_i$$

which can be represented as a relative TRP error as:

Equation 2.10.1.2-3

$$1 + \frac{Error_{TRP}}{TRP} \cong \frac{\frac{\pi}{2NM} \sum_{i=1}^{N-1} \sum_{j=0}^{M-1} [EiRP_{Total}(\theta_i, \phi_j) + Error(\theta_i, \phi_j)] \sin(\theta_i)}{\frac{\pi}{2NM} \sum_{i=1}^{N-1} \sum_{j=0}^{M-1} EiRP_{Total}(\theta_i, \phi_j) \sin(\theta_i)}$$

which simplifies to:

Equation 2.10.1.2-4

$$\frac{Error_{TRP}}{TRP} \cong \frac{\sum_{i=1}^{N-1} \sum_{j=0}^{M-1} Error(\theta_i, \phi_j) \sin(\theta_i)}{\sum_{i=1}^{N-1} \sum_{j=0}^{M-1} EiRP_{Total}(\theta_i, \phi_j) \sin(\theta_i)}$$

In a ripple test, the variation occurs along only one axis of rotation, so it's possible to simplify this equation further. Although either axis could be held constant, the following formulation will assume that the ripple is along the theta axis. The phi axis result is similar.

Substituting in the theta ripple test geometry results in the following equation:

Equation 2.10.1.2-5

$$\frac{Error_{TRP}}{TRP} \cong \frac{\sum_{i=1}^{N-1} Error(\theta_i) \sin(\theta_i)}{\sum_{i=1}^{N-1} EiRP_{Total}(\theta_i) \sin(\theta_i)}$$

Assuming $N > 50$, the expanded uncertainty for a 95% confidence level ($k = 2$) is just:

$$U = 2 u(x)$$

Equation 2.10.1.2-6

The linear representation of the expanded uncertainty is given by:

$$U_{lin} = (1 + s_{max}(p_k))^2 = \left(1 + \sqrt{\frac{1}{(N-1)} \sum_{k=0}^{N-1} \left[\left(\frac{p_k}{\bar{p}} - 1 \right) \sin(\theta_k) \right]^2} \right)^2$$

Equation 2.10.1.2-7

Assume that the relative ripple from the ripple test, $(p_k/\bar{p} - 1)$, is equivalent to the relative error at a given EIRP point, $Error(\theta_i, \phi_j)/EiRP_{Total}(\theta_i, \phi_j)$, so that the theta-axis ripple gives:

Equation 2.10.1.2-8

$$U_{lin} = \left(1 + \sqrt{\frac{1}{(N-1)} \sum_{i=0}^{N-1} \left[\left(\frac{Error(\theta_i)}{EiRP_{Total}(\theta_i)} \sin(\theta_i) \right)^2 \right]} \right)^2$$

We can normalize the $Error/EiRP_{Total}$ ratio such that $EiRP_{Total}$ is one everywhere (equivalent to an isotropic radiator) and define a new error term, as the relative error at each EIRP point. The expanded uncertainty then simplifies to:

Equation 2.10.1.2-9

$$U_{lin} = \left(1 + \sqrt{\frac{1}{(N-1)} \sum_{i=0}^{N-1} [(Error'(\theta_i) \sin(\theta_i))^2]} \right)^2$$

In the limiting case of $Error'(\theta_i) = 0$, this reduces to $U_{lin} = 1$ so that $U = 0$ dB. For an isotropic radiator, the TRP error equation becomes:

Equation 2.10.1.2-10

$$Error'_{TRP} \cong \frac{\sum_{i=1}^{N-1} Error'(\theta_i) \sin(\theta_i)}{\sum_{i=1}^{N-1} \sin(\theta_i)} = \frac{\sum_{i=1}^{N-1} Error'(\theta_i) \sin(\theta_i)}{2(N-1)/\pi}$$

In the limiting case of $Error'(\theta_i) = 0$, this reduces to $Error'_{TRP} = 0$. The corresponding linear value for comparison to the uncertainty is given by $1 + Error'_{TRP}$. When $Error'_{TRP} = 0$, this results in a 0 dB error. It should be noted that the relative error can never be less than -1 since that would imply that $TRP + Error_{TRP} < 0$, which is impossible. Comparing these two formulations gives:

Equation 2.10.1.2-11

$$\left(1 + \sqrt{\frac{1}{(N-1)} \sum_{i=0}^{N-1} [(Error'(\theta_i) \sin(\theta_i))^2]}\right)^2 \text{ and } 1 + \frac{\sum_{i=1}^{N-1} Error'(\theta_i) \sin(\theta_i)}{2(N-1)/\pi}$$

Note the similarities between the two equations.

2.10.2 Effect of Ripple on DUT Measurement for MIMO (Multiple Input Multiple Output)

The uncertainty contribution related to ripple shall be determined using the ripple test described in *CTIA 01.40* [6]. The overall multipath nature of the environment simulation implies that only the average power contribution of the chamber ripple has any direct impact on the measured quantity, so the surface standard deviation measurement uncertainty would apply similar to that for the integrated quantities of TRP and TIS. See Section 2.10.1.1.

2.10.3 Effect of Ripple on Range Reference Measurement

In addition to impacting the DUT results, the Range Reference Measurement can potentially suffer the effects of the signal ripple. Since the range reference measurement may be performed with various support structure components removed, the impact on the measurement uncertainty is based only on the ripple of components remaining in the test volume during the calibration process. The value of the uncertainty component arising from ripple depends on the directivity of the reference antenna, with higher gain antennas typically seeing lower chamber induced ripple, but more uncertainty related to the reference gain and phase center position of the reference antenna.

- Where the Calibrated Reference Antenna is a sleeve dipole or magnetic loop placed in the center of the test volume, the standard uncertainty shall be calculated using the maximum ripple obtained in the phi ripple test procedure outlined in *CTIA 01.73* [2] Sections 5.3.2 and 5.4.2. The data is evaluated at $z = 0$, given that this is the test configuration for the range reference measurement. If the dipole length is less than 300 mm then only one radial position $r = 150 \text{ mm}$ needs to be considered. If the dipole length is above 300 mm then both radial positions ($r = 150 \text{ and } 250 \text{ mm}$) need to be considered. Adjust the measured values using the law of cosines as outlined in *CTIA 01.73* [2] Section 5.7 to account for the path loss variation when the antenna is offset from the center. For each radial position and frequency measured, determine the ripple by taking the difference between the maximum and minimum signal measured in azimuth. Divide this value by 2 to obtain a symmetric value. The standard uncertainty is then obtained by dividing this value by $\sqrt{3}$ since the uncertainty is considered to be rectangularly distributed. For each frequency, use the radial position with the worst case ripple result in the measurement uncertainty budget. In cases where advanced calibration methods are used to minimize this contribution (e.g. ripple or efficiency based calibrations as described in Section 4.6.3 in *CTIA 01.73* [2]), this contribution may be further reduced. For ripple based calibrations the ripple contribution associated with the range calibration may be reduced by fifty percent. For efficiency-based calibration the ripple contribution associated with the range calibration may be replaced by the SSD based ripple.
- Where the Calibrated Reference Antenna is a ridged horn, the maximum ripple is calculated using the maximum and minimum signal (total power, phi and theta) measured following the procedure outlined in Section 5.5 in *CTIA 01.73* [2]. For each radial position determine the difference between the maximum and minimum total power and divide this by 2 to obtain a symmetric value. To calculate the standard uncertainty, divide by $\sqrt{3}$ since the uncertainty is considered to be rectangularly distributed. For each frequency, use the radial position with the worst-case ripple result in the measurement uncertainty budget.

2.11 Quality of the Quiet Zone

2.11.1 Effect on DUT Measurement

The Quality of the Quiet Zone procedure characterizes the quiet zone performance of the anechoic chamber, specifically the effect of reflections within the anechoic chamber including any positioners and support structures. The MU term additionally includes the amplitude variations effect of offsetting the directive antenna array inside a DUT from the center of the quiet zone as well as the directivity MU, i.e., the variation of antenna gains in the different direct line-of-sight links.

2.11.2 Effect on Calibration Stage

During the calibration process the calibration antenna will be placed at the center of the quiet zone. Therefore, only point P1 from the quality of quiet zone procedure (see *CTIA 01.22 [8]*) needs to be considered for the Quality of the Quiet Zone validation measurement.

2.12 Influence of the Ambient Temperature on the Test Equipment

Temperature is the only influence quantity in the tests covered by this test plan. It influences test equipment used for TRP and TIS. This measurement uncertainty must be included when the test equipment is used outside of the certified temperature range.

TRP test

The ambient temperature uncertainty $\pm v$ in Kelvin is converted to a level uncertainty by means of formula 5.2 in *ETSI TR 100 028 [8]* Part 1. The test laboratory making the measurements may, by means of additional measurements, estimate its own influence quantity dependencies, but if this is not carried out the values stated in table F.1 in *ETSI TR 100 028 [8]* Part 2 should be used as worst-case values.

The standard uncertainty shall be calculated as:

$$u_{j \text{ temperature uncertainty}} = \frac{\sqrt{\left(\frac{v_{temp}}{3}\right)^2 \times (\mu_{power_avg})^2 + (\mu_{power_std})^2}}{23} \text{ dB}$$

where

μ_{power_avg} is mean value of power measurement sensitivity in percentage per Kelvin (%/K). A worst-case value is 4 %/K for $k = 2$ (see *ETSI TR 100 028* Part 2 [8]).

μ_{power_std} is standard deviation of power dependence per Kelvin. A worst-case value is 1.2 %/K for $k = 2$ (see *ETSI TR 100 028 [8]* Part 2).

Example of a typical measurement uncertainty calculation: Ambient temperature uncertainty = ± 1 K.

$$u_{j \text{ temperature uncertainty}} = \frac{\sqrt{\left(\frac{1\text{K}}{3}\right)^2 \times ((4\%/K)^2 + (1.2\%/K)^2)}}{23} = 0.10\text{dB}$$

Note: The μ_{power_avg} and μ_{power_std} are used as percentage changes per Kelvin and temperature v_{temp}

in Kelvin.

TIS test

The ambient temperature uncertainty $\pm v$ in Kelvin is converted to a level uncertainty by means of formula 5.2 in *ETSI TR 100 028* [8] Part 1. The test laboratory making the measurements may, by means of additional measurements, estimate its own influence quantity dependencies, but if this is not carried out the values stated in table F.1 in *ETSI TR 100 028* [8] Part 2 should be used as worst-case values.

The standard uncertainty shall be calculated as:

$$u_{j \text{ temperature uncertainty}} = \frac{\sqrt{\left(\frac{(v_{temp})^2}{3}\right) \times ((\mu_{voltage_avg})^2 + (\mu_{voltage_std})^2)}}{11.5} \text{ dB}$$

where

$\mu_{voltage_avg}$ is mean value of voltage measurement in percentage per Kelvin (%/K). A worst-case value is

2.5 %/K for $k = 2$ (see *ETSI TR 100 028* [8] Part 2).

$\mu_{voltage_std}$ is standard deviation of voltage dependence per Kelvin. A worst-case value is 1.2 %/K for $k = 2$ (see *ETSI TR 100 028* [8] Part 2).

Example of a typical measurement uncertainty calculation: Ambient temperature uncertainty = $\pm 3 \text{ K}$.

$$u_{j \text{ temperature uncertainty}} = \frac{\sqrt{\left(\frac{(3[K])^2}{3}\right) \times ((2.5[\%/K])^2 + (1.2[\%/K])^2)}}{11.5} = 0.42 \text{ dB}$$

Note: The $\mu_{voltage_avg}$ and $\mu_{voltage_std}$ are used as percentage changes per Kelvin and temperature v_{temp} in Kelvin.

2.13 Uncertainties Related to Testing with Near Field Phantoms

2.13.1 Estimation of Dielectric Parameter Measurement Uncertainties of Phantoms

The measurement procedures described in this document use vector network analyzers for dielectric property measurements. Network analyzers require calibration in order to account for and remove inherent losses and reflections. The uncertainty budget for dielectric measurement contains inaccuracies in the calibration data, analyzer drift, and random errors. Other sources of errors are the tolerances on the sample holder hardware, and deviations from the optimal dimensions for the specified frequencies, and sample properties and dimensions. This applies regardless of the type of sample holder and the nature of the scattering parameters being measured.

An example uncertainty template is shown in [Table 2.13.1-1](#). Influence quantities shown may or may not apply to a specific test set-up or procedure, and other components not listed may be relevant in some test set-ups. The contributions also depend on the frequency and the type of sample (liquid, gel or solid). Measurement of well-characterized reference materials can be used to estimate the dielectric property measurement uncertainty, as described in the following procedure.

Note: Due to the inability to assess the measurement uncertainty of the solid tissue equivalent material for the head phantom, the use of solid head phantoms is not allowed in the test plan at this time.

1. Configure and calibrate the network analyzer in a frequency span large enough for the frequency range of interest, for example from 300 MHz to 3 GHz in 5 MHz steps, or with five or more frequencies within the device transmission band.
2. Measure a reference material at least n times to obtain the average and standard deviation for the relative permittivity and conductivity at each device center-band and nearby frequencies.
3. For each of the test runs from step 2, to verify calibration validity versus frequency, calculate the differences between the measured and corresponding reference data at five or more frequencies within the device transmission band using the equations.

$$\varepsilon'_r \text{ tolerance} [\%] = 100 \times \left| \frac{\varepsilon'_{r \text{ measured}} - \varepsilon'_{r \text{ ref}}}{\varepsilon'_{r \text{ ref}}} \right|$$

$$\sigma_{\text{tolerance}} [\%] = 100 \times \left| \frac{\sigma_{\text{measured}} - \sigma_{\text{ref}}}{\sigma_{\text{ref}}} \right|$$

4. Use predetermined standard deviations for permittivity and conductivity if available. Otherwise, calculate the standard deviation of the mean (s/\sqrt{n}), e.g., *NIS 81* [9], using the maximum value versus frequency for the n separate permittivity and conductivity tolerances of step 3.
5. Estimate the uncertainties for the other components of [Table 2.13.1-1](#) (and other relevant components if needed) in the frequency range under consideration.
6. The individual uncertainties for ε'_r and σ each are entered into the columns a , b , c of [Table 2.13.1-1](#) to calculate the standard uncertainties u_i and the combined standard uncertainty. Insert a completed version of [Table 2.13.1-1](#) into the test report, along with rationale for which influence quantities were used or omitted.
7. Measure a second reference material to verify relative calibration validity and ascertain that the measured data agrees with the reference values as in step 3. If equipment drift is suspected, go back to the reference material tests of step 2.

Table 2.13.1-1 Example of Uncertainty Template for Dielectric Constant (ϵ_r') or Conductivity (σ) Measurement at a Specific Frequency Band¹

Uncertainty Component	Tolerance/ Uncertainty Value (\pm %)	Probability Distribution	Divisor	C_1	Standard Uncertainty (\pm %)	ν_1 or ν_{eff}
	a		b	c	$u_j = (a/b) \times (c)$	
Repeatability (n repeats, mid-band)		Normal	1^2	1		$n-1$
Reference material ϵ_r' or σ		Rectangular	$\sqrt{3}$	1		∞
Network analyzer drift, linearity, etc.		Rectangular	$\sqrt{3}$	1		∞
Test-port cable variations		U-shaped	$\sqrt{2}$	1		∞
Dimensional accuracy of the sample / line		Normal	1^2	1		∞
Homogeneity of the material		Normal	1^2	1		∞
Temperature of the material		Rectangular	$\sqrt{3}$	1		∞
Combined standard uncertainty						
Expanded uncertainty $k = 2$						

Note 1: Column headings a , b , c are given for reference. Separate tables are usually needed for each ϵ_r' and σ .

Note 2: Assumes the uncertainty value in column a is the standard deviation of a normal distribution. For an expanded uncertainty of a normal distribution, divide by 2.

Uncertainty contributions:

- Repeatability: Refer to evaluation of step 4) above.
- Reference material: Uncertainty of the available reference data.
- Network analyzer: Drift, Linearity and other contributions affecting the capability to measure attenuation and phase at the specific frequency.
- Test-port cable variations: Influence of cable variations on amplitude and phase measurement
- Dimensional accuracy of the sample/line: The reference line is assumed to be an precision 50 Ohm line with a section of air dielectric. With the section of this line filled with the sample material must be well known in length, not change the dimensions of the line, and fill the space without gaps at the inner or outer conductor.
- Homogeneity of the material: Inhomogeneities of the material composition or inclusion of air affects the measurement. S21 or S12 should not differ significantly.
- Temperature of the material: Influence of changes of the dielectric properties of the sample or reference material with the temperature, as far as not compensated.
- Alternative method for evaluating uncertainties can be found in *Dielectric Metrology with Coaxial Sensors* [10].

2.13.2 Uncertainties Related to Testing with Head and Hand Phantoms

This uncertainty component arises from:

- The tolerance of head shape, shell thickness and dielectric parameters and mounting construction
- The tolerance of hand shape and mounting fixture
- Positioning the phone in the hand and the hand with the phone at the head with respect to the definitions provided in *CTIA 01.71* [4]..

The combined uncertainty of head, hand and DUT positioning in the hand and against the head phantoms as defined in *CTIA 01.20* [5] shall be determined as:

Table 2.13.2-1 Standard Uncertainties for the Head, Hand and DUT Positioning in the Hand and Against the Head

Description of Uncertainty Contributions	Standard Uncertainty, dB
Head Phantom Uncertainty	See Section 2.13.2.1
Hand Phantom Uncertainty	See Section 2.13.2.2 and Section 2.13.2.7
Head Phantom Fixture Uncertainty	See Section 2.13.2.4
Hand Phantom Fixture Uncertainty	See Section 2.13.2.4 and Section 2.13.2.7
Phone Positioning Uncertainty	See Section 2.13.2.5 and Section 2.13.2.7
Combined Standard Uncertainty (root-sum-squares)	

2.13.2.1 Uncertainty Related to Head Phantom

The head phantom uncertainty is the effect of the tolerances of the inner and outer surface shape, the dielectric parameters and the shell thickness, as well as the supporting materials except the head phantom fixture. The transformations of these tolerances to uncertainties for TRP/NHPRP/UHRP/PGRP have been studied in *The Uncertainties and Repeatability Limitations of Transmitter and Receiver Performance Assessments Posed by Head Phantoms* [11]. The following approximations (Equation 2.13.2.1-1 through Equation 2.13.2.1-4) shall be used to determine the head uncertainty for both orientations, i.e., vertical and horizontal orientation, where a rectangular distribution shall be assumed:

Equation 2.13.2.1-1

$$u_{head_phantom_shell}[dB] = c_1 \cdot \left[10 \cdot \log_{10} \left(1 + \left| \frac{\Delta d}{d} \right| \right) \right]$$

Equation 2.13.2.1-2

$$u_{head_phantom_permittivity}[dB] = c_2 \cdot \left[10 \cdot \log_{10} \left(1 + \left| \frac{\sqrt{\Delta \epsilon^2 + \Delta \epsilon_{unc}^2}}{\epsilon} \right| \right) \right]$$

Equation 2.13.2.1-3

$$u_{head_phantom_conductivity}[dB] = c_3 \cdot \left[10 \cdot \log_{10} \left(1 + \left| \frac{\sqrt{\Delta \sigma^2 + \Delta \sigma_{unc}^2}}{\sigma} \right| \right) \right]$$

$$u_{head_phantom_shape}[dB] = c_4 \cdot \left[10 \cdot \log_{10} \left(1 + \left| \frac{\Delta shape}{shape} \right| \right) \right]$$

where

The weighting factor $c_1 = 0.10$ as determined according to [Section 3](#) and documented in *The Uncertainties and Repeatability Limitations of Transmitter and Receiver Performance Assessments Posed by Head Phantoms* [11]. Δd is the maximum deviation from the nominal shell thickness d (in [CTIA 01.72](#) [12] from the CAD file, whereas the maximum tolerable deviation is ± 0.2 mm. This tolerance must be verified for an area as wide as ± 50 mm symmetric to the line connecting the Ear Reference Point to the Mouth Point (line extending from the ear reference point to 20 mm below the mouth point as well as for the surface of the ear). The measurements can be conducted with a properly calibrated inductive thickness measurement instrument. The corresponding measurement documentation can be provided by the vendor of the head phantom, which only requires validation if the head phantom has visually degenerated.

$\Delta \varepsilon$ and $\Delta \sigma$ are the tolerances from the target relative permittivity and conductivity of the head material, respectively, where the maximum tolerance shall be $\pm 20\%$. Weighting factor $c_2 = 0.39$ and weighting factor $c_3 = 0.065$ were determined according to the methodology outlined in [Section 3](#).

$\Delta \varepsilon_{unc}$ and $\Delta \sigma_{unc}$ are expanded measurement uncertainties ($k = 2$) of dielectric parameters according to [Section 2.13.1](#).

$\Delta shape$ is the tolerance of the inner surface of the shell. If the tolerance is within 2% from that specified in the SAM CAD file provided in *IEEE 1528-2002* [13] and maintained in this boundary range during the entire measurement cycle, the effect of the head phantom shape can be neglected, i.e., weighting factor

$c_4 = 0$. If the tolerance is larger, a numerical study as outlined in [Section 3](#) must be conducted to determine $\Delta shape$.

When the IEEE SAM head phantom is extended below the neck region, as described in [CTIA 01.72](#) [12] an additional uncertainty of 0.25 dB ($k = 2$) shall be added.

2.13.2.2 Uncertainty Related to Hand Phantom

The hand phantom makes a contribution to OTA measurement uncertainty due to the manufacturing tolerances of its dielectric properties and shape. In this section, the requirements for acceptance of the hands are defined and how the uncertainty of the hands, that meet the minimal requirements, is determined.

The dielectric properties on the surface of the hand may differ from those of its interior, so both are included in the evaluation. The molded exterior surface of the hand shall be measured directly with an open-ended coaxial probe. The interior hand material is evaluated indirectly, by substituting a cube-shaped sample molded from the same material and having some exterior surfaces removed. The full protocol for evaluating the hand phantom material is as follows:

1. Each hand shall be manufactured together with a reference cube of the same material. The sides of the reference cube shall be not less than 40 mm in length.
2. The molded surface on three orthogonal sides of the cube shall be sliced away to a depth of at least 3 mm, in order to expose interior material for evaluation. The remaining three sides of the cube shall be left untreated.
3. Relative permittivity and conductivity shall be measured at ten specified points on the hand exterior surface (see [Figure 2.13.2.2-1](#) through [Figure 2.13.2.2-4](#)), and the exterior averages ($\varepsilon_{ext_{avg}}$, $\sigma_{ext_{avg}}$ 10 points) and standard deviations ($\varepsilon_{ext_{avg}}$, $\sigma_{ext_{avg}}$ 10 points) calculated accordingly. If a non-standard handgrip is used, then

select 10 points on the hand exterior surface similar to those shown in [Figure 2.13.2.2-1](#) through [Figure 2.13.2.2-4](#).

4. Relative permittivity and conductivity shall be measured at ten different points on each of the three cut, exposed surfaces of the reference cube, and the combined interior averages ($\varepsilon_{int_{avg}}$, $\sigma_{int_{avg}}$ 30 points) and standard deviations ($\varepsilon_{int_{std}}$, $\sigma_{int_{std}}$ 30 points) shall be calculated. Individual interior averages for each of these three sides (ε_{int_i} , σ_{int_i} 30 points) shall also be calculated.
5. The total averages (ε_{avg} , σ_{avg}) shall be calculated as the average of exterior and interior values by either evaluating all data points or using:

$$\left(\varepsilon_{avg} = \frac{\varepsilon_{ext_{avg}} + 3 \cdot \varepsilon_{int_{avg}}}{4}, \sigma_{avg} = \frac{\sigma_{ext_{avg}} + 3 \cdot \sigma_{int_{avg}}}{4} \right)$$

6. The total standard deviations (ε_{std} , σ_{std}) shall be calculated as the statistical combination of exterior and interior values by either evaluating all data points or using:

$$\varepsilon_{std} = \sqrt{\frac{1}{4} \left(\varepsilon_{ext_{std}}^2 + \varepsilon_{ext_{avg}}^2 + 3 \cdot \left(\varepsilon_{int_{std}}^2 + \varepsilon_{int_{avg}}^2 \right) \right) - \varepsilon_{avg}^2}$$

$$\sigma_{std} = \sqrt{\frac{1}{4} \left(\sigma_{ext_{std}}^2 + \sigma_{ext_{avg}}^2 + 3 \cdot \left(\sigma_{int_{std}}^2 + \sigma_{int_{avg}}^2 \right) \right) - \sigma_{avg}^2}$$

7. The hands are acceptable, i.e., meeting the minimal requirements, if:
 - a. ε_{avg} deviate by less than 15% from the target values
 - b. σ_{avg} deviate by less than 25% from the target values
 - c. the difference between the averaged permittivity of each 10-point interior surface ($\varepsilon_{int_{avg}}$) deviates by less than 10% and ($\varepsilon_{ext_{avg}}$) by less than 20% from the total average ε_{avg} .
 - d. the difference between the averaged conductivity of each 10-point interior surface ($\sigma_{int_{avg}}$) deviates by less than 20% and ($\sigma_{ext_{avg}}$) by less than 30% from the total average σ_{avg} .
 - e. the standard deviation of the combined measurements (30 interior points and 10 exterior points) is less than 20% for permittivity ε_{std} and less than 40% for conductivity σ_{std}
8. For the hands meeting the minimal requirements of step 7, the following approximations ([Equation 2.13.2.2-1](#) through [Equation 2.13.2.2-3](#)) shall be used to determine the hand uncertainty where a rectangular distribution is assumed. The total standard uncertainty (root-sum-squares of $u_{hand_phantom_permittivity}$, $u_{hand_phantom_conductivity}$, $u_{hand_phantom_shape}$) shall not exceed 0.5 dB:

Equation 2.13.2.2-1

$$u_{hand_phantom_permittivity}[dB] = c_1 \cdot \left[10 \cdot \log_{10} \left(1 + \left| \frac{\sqrt{\Delta\varepsilon_{avg}^2 + \varepsilon_{unc}^2 + (a_1 \varepsilon_{std})^2}}{\varepsilon} \right| \right) \right]$$

Equation 2.13.2.2-2

$$u_{hand_phantom_conductivity}[dB] = c_2 \cdot \left[10 \cdot \log_{10} \left(1 + \left| \frac{\sqrt{\Delta\sigma_{avg}^2 + \sigma_{unc}^2 + (a_1 \sigma_{std})^2}}{\sigma} \right| \right) \right]$$

Equation 2.13.2.2-3

$$u_{hand_phantom_shape}[dB] = c_3 \cdot \left[10 \cdot \log_{10} \left(1 + \left| \frac{\Delta shape}{shape} \right| \right) \right]$$

whereby,

$\Delta\varepsilon_{avg}$, $\Delta\sigma_{avg}$, ε_{std} , σ_{std} are the values determined as defined above and ε_{unc} and σ_{unc} are expanded measurement uncertainties ($k = 2$) of the dielectric parameters according to Section 2.13.1 determined for homogeneous materials.

The cube will be provided together with the hand such that the user can evaluate if the interior (cube) properties of the hand has degenerated over time by performing the test above. $c_1 = 0.78$, $c_2 = 0.39$ and $a_1 = 0.50$ were determined according to the methodology outlined in Section 3. OCP measurements at the surface of used hands may change over time with minimal impact on OTA evaluations due to the sensitivity of the OCP method on surface contamination.

$\Delta shape$ is the uncertainty on TRP/NHPRP/UHRP/PGRP, resulting from the tolerance of the hand phantom shape. Since the hands are usually manufactured within models, the tolerance is 2% and therefore the effect is negligible, i.e., $c_3 = 0$. If the tolerance is larger, a numerical study as outlined in Section 3 must be conducted to determine $\Delta shape$.

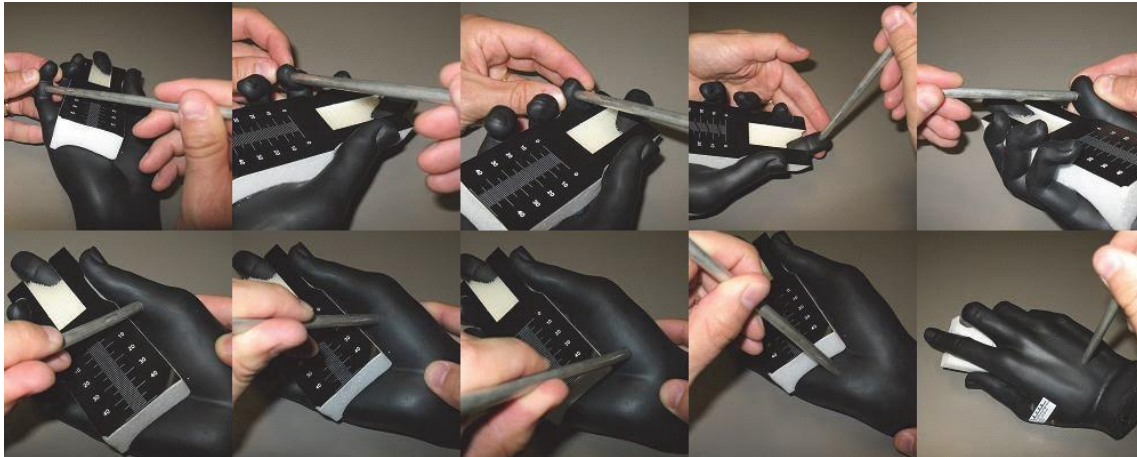


Figure 2.13.2.2-1 Ten Locations of Dielectric Measurements at the Brick Hand Surface



Figure 2.13.2.2-2 Ten Locations of Dielectric Measurements at the Fold Hand Surface



Figure 2.13.2.3-3 Ten Locations of Dielectric Measurements at the Narrow Data Hand Surface



Figure 2.13.2.2-4 Ten Locations of Dielectric Measurements at the PDA Hand Surface

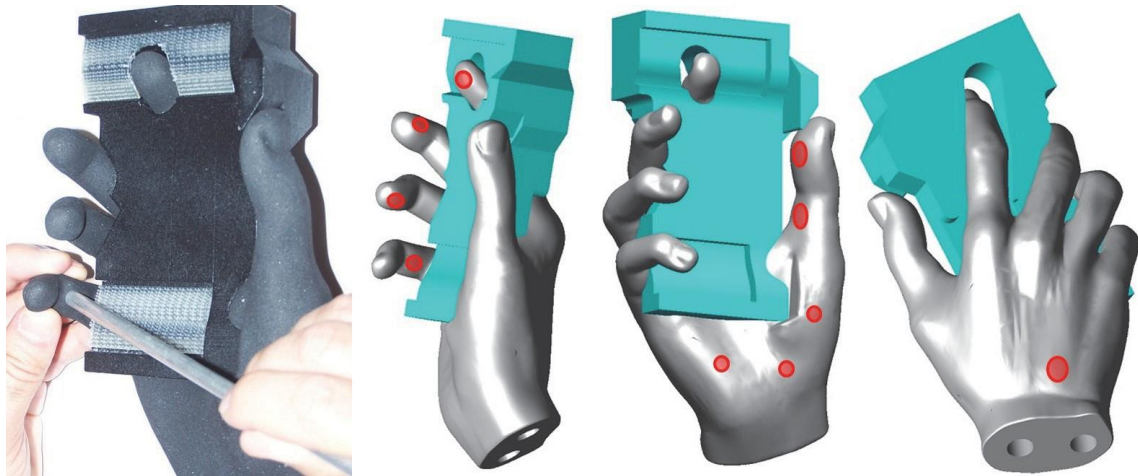


Figure 2.13.2.2-5 Ten Locations for Dielectric Measurement of the Wide Grip Hand Surface

2.13.2.3 Evaluation of Uncertainty Related to Fixture, Hand and DUT Positioning

The uncertainty components related to phantom testing can be determined numerically, e.g., by the phantom vendors, or through experimentation. They shall represent the maximum uncertainty for TRP and TIS measurements.

The measurement uncertainty estimate shall include the following frequency bands:

- 600-1176.45 MHz
- 1176.45-2200 MHz
- 2300-2800 MHz
- 3300-3800 MHz
- 5000-6000 MHz

The selected phones used in the evaluation shall be used to represent the uncertainty of the entire phone population. Since the evaluation effort per phone can be significant, the total number of phones used in the evaluation is limited for practical reasons. Worst-case considerations combined with statistical methods shall be applied. For guidance, see *NIST* [14]. For the 600-1176.45 MHz and 1176.45-2200 MHz bands, the number of phones shall be at least eight and include:

- 2 monoblock phones with width between 40-56 mm (fixed or portrait slides) [e.g. fitting in the monoblock hand phantom]
- 2 fold phones [e.g. fitting in the fold hand phantom]
- 2 monoblock phones with width between 56-72 mm [e.g. fitting in the PDA grip hand phantom]
- 2 monoblock phones with width between 72-92 mm [e.g. fitting in the wide grip hand phantom]

Preferably, at least one phone should have an antenna at the base of the phone, one should have an extended antenna, and one phone should have an antenna embedded in the back of the phone.

For the 2300-2800 MHz, 3300-3800 and 5000-6000 bands, at least four phones shall be used and include:

- 2 monoblock phones with width between 56-72 mm [e.g. fitting in the PDA grip hand phantom]
- 2 monoblock phones with width between 72-92 mm [e.g. fitting in the wide grip hand phantom]

All phones may have embedded antennas. Preferably, at least one phone should have an antenna at the base of the phone and one phone should have an antenna embedded in the back of the phone.

The phones for all bands should be significantly different in size and have antennas located in different locations within the phone. All phones used in the study should be well characterized and known to be stable.

The applied evaluation techniques, the rationale for the selection of phones and frequencies, obtained results and extrapolations for obtaining the required coverage factors shall be documented and made available to the reviewing bodies.

2.13.2.4 Uncertainty Related to Head and Hand Phantom Fixtures

The head and hand phantom fixtures uncertainty is the effect of the head and hand phantom fixtures on the TRP/NHPRP/UHRP/PGRP compared to the standard configuration with an ideally RF transparent fixture. The head phantom fixture is the adapter between the mounting structure or head adapter connected to the turntable and head. The hand fixture is the fixture with which the hand with the phone can be appropriately positioned at the head. They shall be constructed with low-loss dielectric material with a dielectric constant of less than 5 and a loss tangent of less than 0.05 for frequencies between 300 MHz-6 GHz and the proof of compliance has to be documented (these material parameters can be determined using the methods described in *CTIA 0.72 [12]*). Any metallic parts such as screws shall not exceed 10 mm in any dimensions. The head and hand phantom fixtures and the mounting structure can be evaluated combined or separately, as described in Section 2.13.2.4.1 and Section 2.13.2.4.2. Two methods, an experimental and a numerical technique, are proposed to obtain an uncertainty estimate. If the uncertainties are evaluated individually the combined uncertainty shall be determined by root-sum-squares since the directional distortions can be considered independent. The effect of the fixture is frequency dependent and shall be evaluated (at a minimum) at the middle channel of the 1) 5 GHz 802.11n band (the middle channel will be the channel supported from this list (44, 60, 120, 157, 165) that is closest to 5500 MHz), 2) 3GPP Band 48, 3) 3GPP Band 41 or 3GPP Band 7, 4) PCS band and 5) Cell band in order to estimate the uncertainty of the 5000-6000 MHz, 3300-3800 MHz, 2300-2800 MHz, 1175.45-2200 MHz and the 600-1175.45 MHz bands, respectively.

2.13.2.4.1. Experimental Evaluation

The following procedure allows evaluation of the RF impact of any additional support structure or fixtures used to hold the hand phantom against the side of the head phantom. Repeated TRP tests with and without the fixtures in place are used to estimate the resulting measurement uncertainty using a Type A analysis.

For the purpose of this test it is necessary to rigidly attach each phone and hand combination to the head in order to evaluate the TRP with and without the supporting fixture in place. This may be accomplished using a minimum of cellophane tape and expanded polystyrene foam as required to support the phone and hand, while avoiding significant impact on the radiation pattern of the DUT. In order to provide sufficient variation in radiation pattern and near-field coupling effects, the minimum number and type of DUTs, as specified in Section 2.13.2.3, shall be used.

The RF evaluation shall be performed at the middle channel of the 1) 5 GHz 802.11n¹ band (the middle channel will be the channel supported from this list (44, 60, 120, 157, 165) that is closest to 5500 MHz),

3GPP Band 48, 3) 3GPP Band 41 or 3GPP Band 7, 4) PCS band and 5) Cell band in order to estimate the uncertainty of the 5000-6000 MHz, 3300-3800 MHz, 2300-2800 MHz, 1175.45-2200 MHz and the 600-1175.45 MHz bands, respectively.

For each phone, repeat the following steps:

1. Record the phone model, style, description, serial number, and any other identifying information.
2. Set up and verify proper operation of the OTA test system.

3. Mount the phone in the appropriate hand phantom and attach rigidly to the head phantom as described in *CTIA 01.71 [4]* and place the head/hand/phone combination in the test system.
4. Perform a TRP test at each required channel, repeating the test three times.
5. Install the hand support structure, positioning it in a manner representative of the way it would be oriented in order to hold the hand phantom in its current position, taking care to avoid moving the hand phantom and phone relative to the head phantom.
6. Measure the TRP of the head/hand/phone/fixture combination at each required channel and repeat the test a total of five times.
7. Remove the hand support structure and repeat the TRP test on the head/hand/phone combination an additional three times.
8. Calculate the TRP and NHPRP values for each measurement as specified in *CTIA 01.90 [15]*, as well as the UHRP (Upper Hemisphere Radiated Power) and PGRP (Partial GNSS Radiated Power) corresponding to the UHS and PIGS values.
9. For each test frequency, determine the average and standard deviation of each value across the six head/hand/phone only tests.
10. Subtract the average values from the corresponding values for each of the head/hand/phone/ fixture tests and determine the absolute maximum of each value.

Once each phone has been tested in this manner, perform the following analysis to determine the uncertainty estimate for this support fixture.

1. Determine the maximum of each TRP/NHPRP/UHRP/PGRP delta across all phones.
2. Convert each of these values, X_{Max} , to a standard uncertainty assuming a rectangular distribution:

$$\left(u_{X_{Maxj}} = X_{Max}/\sqrt{3}\right)$$

3. Average the standard deviation of each TRP/NHPRP/UHRP/PGRP across all reference (head/hand/phone only) tests. This value represents the standard uncertainty inherent in the repeatability of the test system.
4. Determine the standard uncertainty of each TRP/NHPRP/UHRP/PGRP value using the following formula:

$$u_{Xj} = \sqrt{u_{X_{Maxj}}^2 - \sigma^2}$$

In the event that $u_{X_{Maxj}}$ is less than the repeatability standard uncertainty σ , then

$$u_{Xj} = 0$$

5. The maximum u_{Xj} from the TRP/NHPRP/UHRP/PGRP values shall then be used as the standard measurement uncertainty estimate, u_p , for the fixture. If the maximum u_{Xj} , u_{XjMax} , is less than the average of all σ for the various radiated power quantities at a given frequency, σ , (indicating that the effect of the support structure cannot be clearly extracted from the noise of the repeatability) then the required u_j shall be given by the following formula:

$$u_j = \sqrt{\frac{u_{XjMax}^2 + \sigma^2}{2}}$$

2.13.2.4.2. Numerical Evaluation

The study shall be conducted according to [Section 3](#) by comparing the differences between TRP/NHPRP/UHRP/PGRP with and without fixtures.

2.13.2.5 Uncertainty Related to Phone Positioning

The phone positioning is the largest phantom related uncertainty and requires careful assessment, especially since it depends on the skills and care of the person conducting the tests. The position of the phone affects the electromagnetic loading with respect to the hand and head, the scattering and absorption properties, orientation with respect to the evaluation plan, etc. The effect of this tolerance on TRP/NHPRP/UHRP/PGRP not only depends on the deviation of the position, but also depends strongly on the phone and frequency. Two methods, an experimental and a numerical technique, are proposed to obtain an uncertainty estimate based on a maximum expected position variation. In order to determine this maximum position variation, the lab must evaluate how their personnel place the DUT on the phantom(s) using any available fixturing, as well as any flexure in their test setup that can cause the position to vary, and then use that maximum positional variation to determine the overall RF impact of the expected variation.

To determine the expected positioning repeatability by the lab technicians a variety of different phone styles, shapes, and sizes shall be evaluated. The minimum number and type of phones, as described in Section 2.13.2.3 shall be evaluated.

For each phone, perform the following steps:

1. Instruct each technician to attach the phone to the head and hand as directed in *CTIA 01.71 [2]* using whatever fixturing is to be used regularly. The technician shall not be “coached” to produce the best setup, although prior training to ensure that the technicians are aware of the proper methodology is recommended.
2. For all phone setups, have an independent observer record the position of the phone relative to the available reference marks on the head and/or hand phantom, as well as the position of the hand relative to the head, when applicable. Recorded information should represent both position offsets in h and v directions and the angular rotations r_1 and r_2 (Figure 2.13.2.5.1-1). It is recommended that a repeatable system of photography (e.g., camera(s) on tripod(s) at unchanged or precisely marked locations relative to the head/hand) be used to photograph each setup to allow overlaying the various photographs to evaluate the range of variation in position/orientation from multiple directions (e.g., top, front, and side).
3. For systems where the head/hand combination rotates around a horizontal axis, such that the effect of gravity on the mounting will change throughout the test, the variation in mounting position shall be evaluated as a function of orientation. In this case, mount the head/hand/DUT combination as used and compare the relative positions of the DUT and hand at no less than four positions (every 90° in an above, below, left, right orientation)
4. Repeat steps 1-3 for each technician in the lab, ensuring that each mounting process is started from the same completely disassembled state. For labs with a small number of technicians, the mounting should be repeated multiple times by each technician to produce at least five separate mountings per phone.
5. Repeat steps 1-4 for all technicians.
6. For each phone, determine the maximum deviation from the target reference points described in *CTIA 01.71 [2]* and treat it as a rectangular quantity for each measured dimension h , v , r_1 and r_2 . If the sample size is sufficiently large and it has been shown that the distribution is normal, then the standard deviation can be assessed and used in the following evaluation of Section 2.13.2.5.2.

In the case where the RF evaluation will be performed on equivalent phone models to those evaluated here, the corresponding variation quantities for each phone model may be used. Otherwise, the maximum variation across all evaluated phone models shall be used for the RF uncertainty evaluation. It is recommended that this procedure is repeated whenever a technician is added to the team.

For relative measurements, if the phone is not handled between measuring both test configurations, then the additional uncertainty due to the positioning error of the DUT with the head/hand phantom will be 0.00 dB for this measurement. Otherwise, this uncertainty should be included twice, once in the reference TRP/TIS measurement, and once in the relative measurement.

2.13.2.5.1. Experimental Evaluation

The following procedure allows evaluation of the RF impact of the expected positioning uncertainty based on the analysis performed above. Repeated TRP tests with intentional deviations matching those found in the previous analysis shall be used, using any corresponding fixturing, etc. In order to provide sufficient variation in radiation pattern and near-field coupling effects, the minimum number and types of DUTs, as described in Section 2.13.2.3, shall be used.

The RF evaluation shall be performed at the middle channel of the 1) 5 GHz 802.11n² band (the middle channel will be the channel supported from this list (44, 60, 120, 157, 165) that is closest to 5500 MHz),

3GPP Band 48, 3) 3GPP Band 41 or 3GPP Band 7, 4) PCS band and 5) Cell band in order to estimate the uncertainty of the 5000-6000 MHz, 3300-3800 MHz, 2300-2800 MHz, 1175.45-2200 MHz and the 600-1175.45 MHz bands, respectively.

For each phone, repeat the following steps:

1. Record the phone model, style, description, serial number, and any other identifying information.
2. Set up and verify proper operation of the OTA test system.
3. Mount the phone in the appropriate hand phantom and attach to the head phantom as described in *CTIA 01.71* [2], offsetting the phone from the target position by the maximum offsets as determined according to Section 2.13.2.5 step 6.
4. Place the head/hand/phone combination in the test system and measure the TRP at each required channel.
5. Choose the maximum deviation dimension and adjust the phone/hand combination so that it is offset in the opposite direction (reverse the sign of the deviation) and repeat step 4.
6. Choose the next largest deviation and repeat the adjustment for that dimension and repeat step 4.
7. Flip the sign on the first deviation again to put that offset back to its starting position and repeat step 4. At this point, four cardinal positions with the maximum deviation shall have been tested.
8. Continue swapping the sign of the remaining deviation quantities, adjusting the position of the phone, and remeasuring the TRP until no less than six distinctly different positions with the maximum position variation have been evaluated.
9. Calculate the TRP and NHPRP values for each measurement as specified in *CTIA 01.90* [15] as well as the UHRP and PGRP corresponding to the UHIS and PIGS values.
10. For each test frequency, determine the maximum delta in dB of each value across the six (or more) head/hand/phone tests.

Once each phone has been tested in this manner, perform the following analysis to determine the uncertainty estimate for the positioning repeatability.

11. For each test frequency, determine the maximum of each TRP/NHPRP/UHRP/PGRP delta in dB across all phones and calculate the standard uncertainty ($k = 1$) due to positioning error using the following formula:

$$u_{\text{positioning}}[\text{dB}] = \frac{u_{\text{positioning_max}}[\text{dB}]}{2\sqrt{3}}$$

2.13.2.5.2. Numerical Evaluation

Alternatively, a Type A uncertainty analysis can be conducted using high-end simulation tools supporting scripting of mechanical positioning. A similar procedure, as described in section 2.13.2.5.1, was performed with all OTA measurements replaced with simulation results. A mechanical position matrix is derived for which the analysis is conducted following the procedures described in Section 3.

The following approximation (Equation 2.13.2.5.2-1) shall be used to determine the phone positioning uncertainty:

Equation 2.13.2.5.2-1

$$u_{\text{positioning}}[\text{dB}] = \sqrt{(k_1 \cdot |h|)^2 + (k_2 \cdot |v|)^2 + (k_3 \cdot |r_1|)^2 + (k_4 \cdot |r_2|)^2}$$

h is the horizontal deviation (see Figure 2.13.2.5.1-1) in mm from the exact position described in CTIA 01.71 [4] and must be determined according to the procedure defined below.

v is the vertical deviation (see Figure 2.13.2.5.1-1) in mm from the exact position described in CTIA 01.71 [4] and must be determined according to the procedure defined below.

r_1 and r_2 are angular deviations (see Figure 2.13.2.5.1-1) in degrees from the exact position described in CTIA 01.71 [4] and must be determined according to the procedure defined below.

$k_1 = 0.18$, $k_2 = 0.07$, $k_3 = 0.14$ and $k_4 = 0.44$ are the sensitivity factors which were determined according to the methodology outlined in Section 3. The maximum sensitivity has been expanded by the number of degrees of freedom. If the maximum deviations for h , v , r_1 and r_2 are determined according to Section 2.13.2.5 step 6, then a rectangular distribution (divisor = 1.73) shall be used. If h , v , r_1 and r_2 are determined as standard deviations assuming a normal distribution. In this case, the standard deviation shall be treated as a standard uncertainty (divisor = 1) shall be used in Table 2.13.2.6-1. These equations are only valid for h and $v \leq 5$ mm and r_1 and $r_2 \leq 2^\circ$.

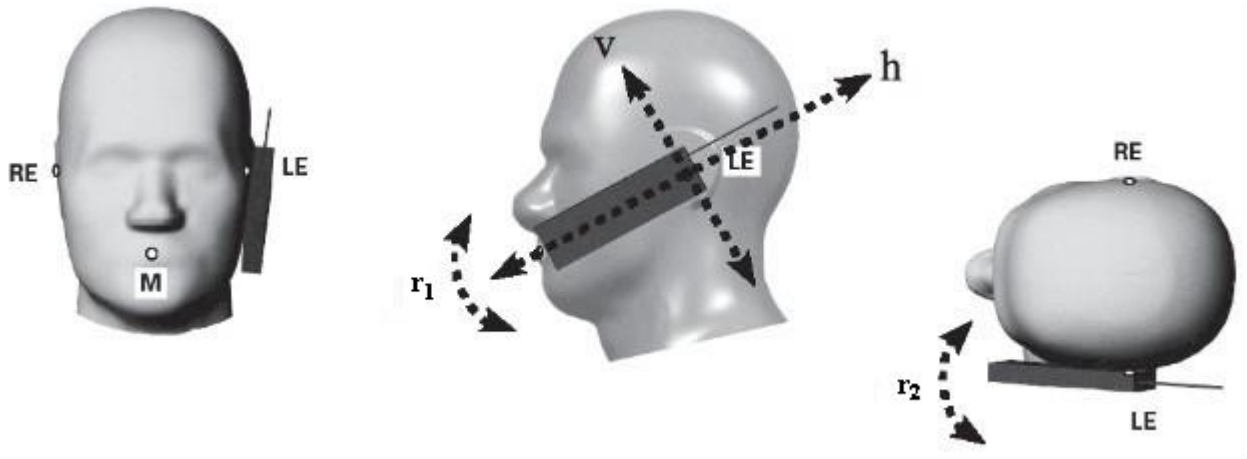


Figure 2.13.2.5.1-1 Phone Positioning Uncertainty Components

2.13.2.6 Example of Uncertainty for Reasonably Worst-case Head, Hand and DUT Positioning in the Hand and against the Head (Informative)

The uncertainty for reasonably worst-case head, hand and DUT positioning in the hand and against the head are provided in Table 2.13.2.6-1.

Table 2.13.2.6-1 Example of Uncertainty Assessment for Reasonably Worst-Case Head, Hand and DUT Positioning in the Hand and Against the Head

Uncertainty Component	Tolerance/ Uncertainty Value	Probability Distribution	Divisor	c_i	Standard Uncertainty (\pm dB)	V_i or V_{eff}
	a		b			
Head Phantom						
Shell Thickness	0.41	Rectangular	1.73	0.10	0.02	∞
Filling/Liquid Dielectric Constant	0.46	Rectangular	1.73	0.39	0.10	∞
Filling/Liquid Conductivity	0.81	Rectangular	1.73	0.065	0.03	∞
Geometry/Shape	1.00	Rectangular	1.73	0.00	0.00	∞
Supporting Structure Uncertainty		Rectangular				
Combined Head Phantom Uncertainty					0.11	
Hand Phantom						
Material Dielectric Constant	0.59	Rectangular	1.73	0.78	0.26	
Material Conductivity	1.10	Rectangular	1.73	0.39	0.25	
Geometry/Shape (incl. spacer)	1.00	Rectangular	1.73	0.00	0.00	
Combined Hand Phantom Uncertainty					0.36	
Fixtures						
Head Phantom Fixture	0.25	Rectangular	1.73	1.00	0.14	
Hand Phantom Fixture	0.40	Rectangular	1.73	1.00	0.23	
DUT Related						
DUT Positioning	0.58	Rectangular	1.73	1.00	0.33	
Combined Standard Uncertainty (Head+Hand+Fixture)					0.57	

Head Phantom				
	Δd	d	a	Reference Equation 2.13.2.1-1
Shell Thickness Uncertainty Component	0.2	2	0.41	
	$\Delta\varepsilon/\varepsilon$	$\Delta\varepsilon_{unc}/\varepsilon$	a	Reference Equation 2.13.2.1-2
Filling/Liquid Dielectric Constant	0.1	0.05	0.46	
	$\Delta\sigma/\sigma$	$\Delta\sigma_{unc}/\sigma$	a	Reference Equation 2.13.2.1-3
Filling/Liquid Conductivity	0.2	0.05	0.81	

Hand Phantom						
	$\Delta\varepsilon_{avg}/\varepsilon$	$\varepsilon_{unc}/\varepsilon$	$\varepsilon_{std}/\varepsilon$	a_1	a	Reference Equation 2.13.2.2-1
Material Dielectric Constant	0.1	0.03	0.2	0.5	0.59	
	$\Delta\sigma_{avg}/\sigma$	σ_{unc}/σ	σ_{std}/σ	a_1	a	Reference Equation 2.13.2.2-2
Material Conductivity	0.2	0.05	0.4	0.5	1.10	

DUT Related						
	h (mm)	v (mm)	r_1 (deg)	r_2 (deg)(deg)	a	Reference Equation 2.13.2.5.2-1
DUT Positioning	2.5	2	2	0.5	0.58	

2.13.2.7 Uncertainties Related to Testing in Data Mode

The hand phantom uncertainty shall be evaluated according to Section 2.13.2.2. The hand phantom data mode fixture uncertainty shall be evaluated according to Section 2.13.2.4. If the uncertainty of positioning of the phone inside the hand is less than ± 1 mm, then this uncertainty is negligible. Otherwise, it shall be evaluated according to Section 2.13.2.5. DUT (including hand phantom) positioning/repositioning uncertainty is performed according to Section 2.17.

Table 2.13.2.7-1 Example of Uncertainty Assessment for Hand Phantom, Fixture and Phone Positioning in Data Mode Testing

Uncertainty Component	Tolerance/ Uncertainty Value	Probability Distribution	Divisor	c_i	Standard Uncertainty (\pm dB)	v_i or v_{eff}
	a		b	c	$u_i = (a/b) \times (c)$	
Hand Phantom						
Material Dielectric Constant	0.59	Rectangular	1.73	0.10	0.26	∞
Material Conductivity	1.10	Rectangular	1.73	0.39	0.25	∞
Geometry/Shape (incl. spacer)	1.00	Rectangular	1.73	0.00	0.00	∞
Combined Hand Phantom Uncertainty					0.36	
Fixture						
Hand Phantom Fixture	0.16	Rectangular	1.73	1	0.09	∞
DUT Related						
DUT Positioning inside Hand Phantom	0	Rectangular	1.73	1	0.00	∞
DUT (including Hand Phantom) Positioning	0	Rectangular	1.73	1	0.00	∞
Combined standard uncertainty (Hand+Fixture)					0.37	

2.13.3 Uncertainties Related to Testing with Forearm Phantom Testing

Uncertainty arises from:

- The tolerance of the forearm shape and dielectric properties
- Positioning the wrist-worn device on the forearm phantom with respect to the definitions provided in section 2.3 of CTIA 01.71 [4].

The combined uncertainty of forearm, and DUT positioning on the forearm phantom shall be determined as follows:

Table 2.13.3-1 Standard Uncertainties for the Forearm, and DUT Positioning on the Forearm

Description of Uncertainty Contributions	Standard Uncertainty, dB
Forearm Phantom Uncertainty	See Section 2.13.3.1
Wrist-worn Device Positioning Uncertainty	See Section 2.13.3.2

2.13.3.1 Uncertainty Related to Forearm Phantom

This uncertainty shall be determined using the method described in Section 2.13.2.2 except that the method is applied to the forearm phantom instead of a hand phantom.

When measuring the relative permittivity and conductivity, refer to Table 2.13.3-1 for the coordinates of twelve test locations defined for forearm phantoms, positioned relative to the coordinate system specified in Figure 2.13.3.1-1. Figure 2.13.3.1-2 highlights the test points on each face of the phantom.

For the forearm phantoms meeting the minimal requirements defined in Section 2.13.2.2, the approximations given in this section shall be used to determine the forearm uncertainty where a rectangular distribution is assumed. The constants, c_1 , c_2 and a_1 were determined for forearm phantoms according to the methodology outlined in Section 3 to be $c_1 = 0.71$, $c_2 = 0.42$ and $a_1 = 0.50$.

As used in Equation 2.13-4, $\Delta shape$ is the uncertainty on TRP, resulting from the tolerance of the forearm phantom $\Delta shape$. Since the forearms are usually manufactured with molds, the tolerance is 2% and therefore the effect is negligible, i.e., $c_3 = 0$. If the tolerance is larger, a numerical study as outlined in Section 3 must be conducted to determine $\Delta shape$.

The total standard uncertainty (root-sum-squares of $u_{forearm\ phantom\ permittivity}$, $u_{forearm\ phantom\ conductivity}$, $u_{forearm\ phantom\ shape}$) shall not exceed 0.5 dB.

Equation 2.13.3.1-1

$$u_{forearm_permittivity}[\text{dB}] = c_1 \cdot \left[10 \cdot \log_{10} \left(1 + \left| \frac{\sqrt{\Delta \varepsilon_{avg}^2 + \varepsilon_{unc}^2 + (a_1 \varepsilon_{std})^2}}{\varepsilon} \right| \right) \right]$$

Equation 2.13.3.1-2

$$u_{forearm_conductivity}[\text{dB}] = c_2 \cdot \left[10 \cdot \log_{10} \left(1 + \left| \frac{\sqrt{\Delta \sigma_{avg}^2 + \sigma_{unc}^2 + (a_1 \sigma_{std})^2}}{\sigma} \right| \right) \right]$$

Equation 2.13.3.1-3

$$u_{forearm_phantom_shape}[\text{dB}] = c_3 \cdot \left[10 \cdot \log_{10} \left(1 + \left| \frac{\Delta shape}{shape} \right| \right) \right]$$

whereby,

$\Delta \varepsilon_{avg}$, $\Delta \sigma_{avg}$, ε_{std} , σ_{std} are the values determined as defined above and ε_{unc} and σ_{unc} are expanded measurement uncertainties ($k = 2$) of the dielectric parameters according to Section 2.13.1 determined for homogeneous materials.

Table 2.13.3.1-1 Coordinates of Ten Locations for Dielectric Measurements on the Forearm Phantom

Point	X (mm)	Y (mm)	Z (mm)
P1	Front Face	0	70
P2	Front Face	-15	35
P3	Front Face	15	15
P4	Front Face	-15	-15
P5	Front Face	15	-65
P6	Back Face	0	70
P7	Back Face	15	35
P8	Back Face	-15	15
P9	Back Face	15	-15
P10	Back Face	-15	-65
P11	0	Right Face	-15
P12	0	Left Face	15

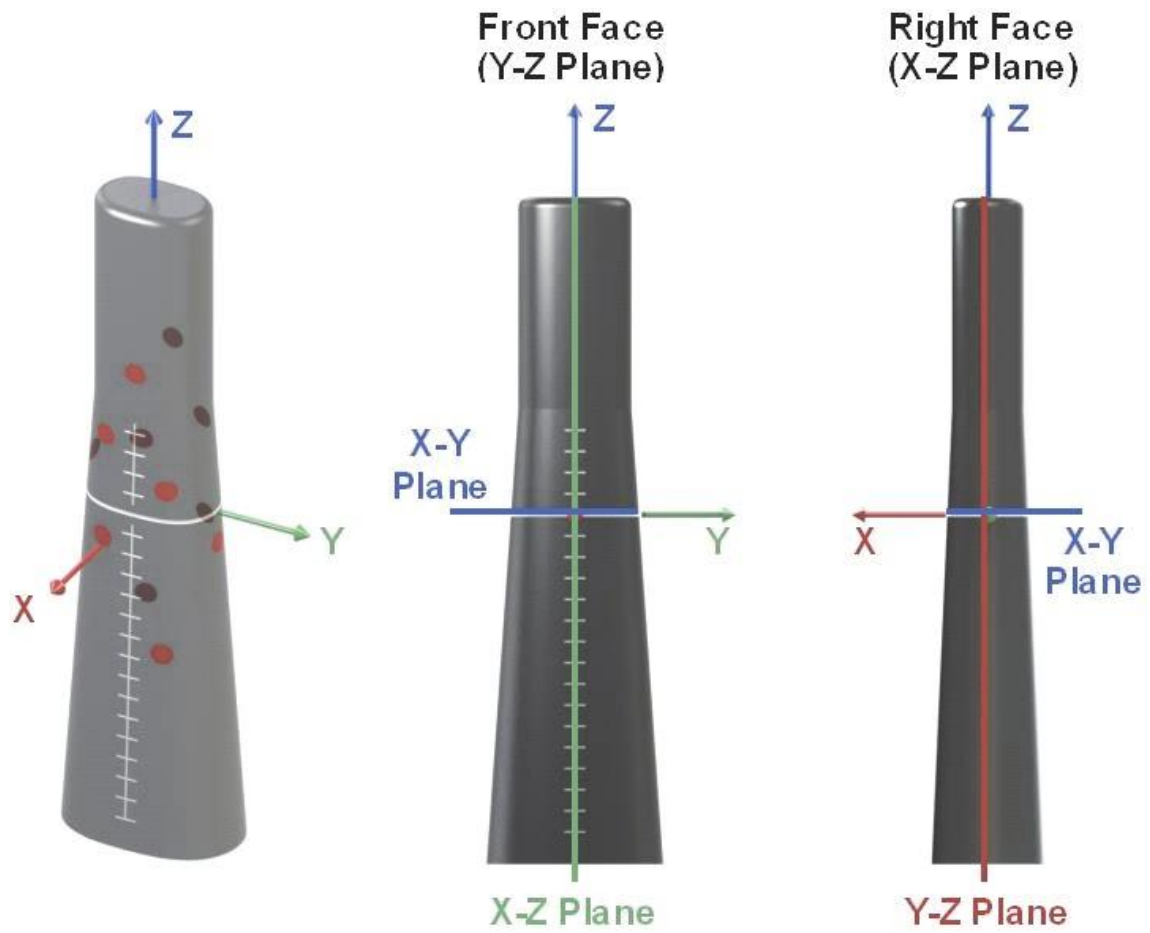


Figure 2.13.3.1-1 Coordinate System for Dielectric Test Locations

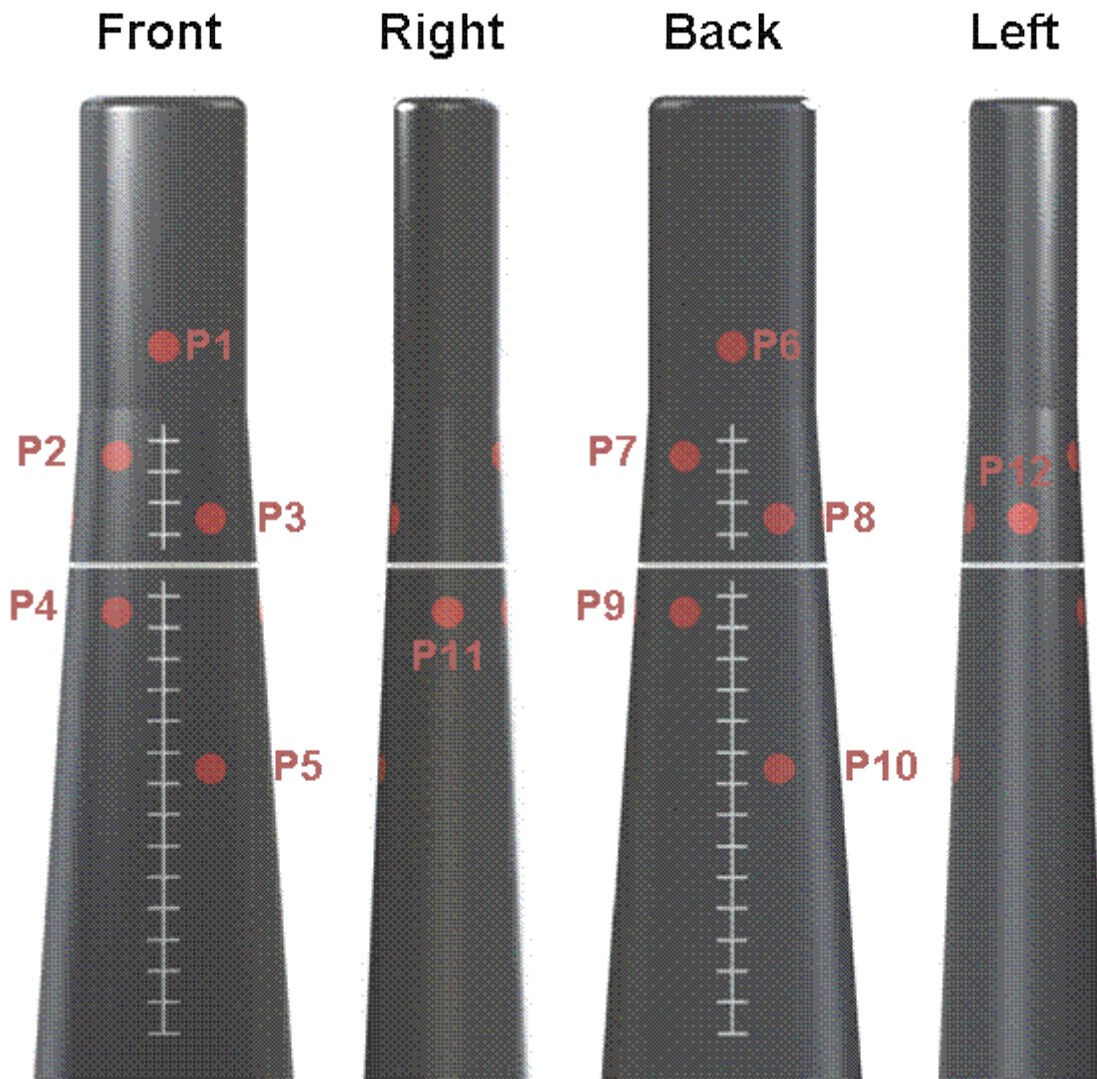


Figure 2.13.3.1-2 Twelve Locations for Dielectric Measurements on the Forearm Phantom

2.13.3.2 Uncertainty Related to Wrist-worn Device Positioning

This uncertainty shall be determined using the method described in Section 2.13.2.5 except that the method is applied to the forearm phantom instead of a hand phantom.

When recording the position of the DUT relative to the available reference marks on the forearm phantom (Section 2.13.2.5 step 2), include position offsets in directions f and g and angular rotations r_1 , r_2 and r_3 shown in Figure 2.13.3.2-1. A numerical evaluation of the wrist-worn device positioning uncertainty was performed.

Based on the numerical evaluation, a similar approximation to that given for hands phantoms shall be used to determine the forearm phantom positioning uncertainty:

Equation 2.13.3.2-1

$$u_{\text{positioning}}[\text{dB}] = \sqrt{(k_1 \cdot |f|)^2 + (k_2 \cdot |g|)^2 + (k_3 \cdot |r_1|)^2 + (k_4 \cdot |r_2|)^2 + (k_5 \cdot |r_3|)^2}$$

where: f is the deviation in mm along the f -axis from the exact position and must be determined according to the procedure defined below. The f -axis is in the X-Y plane, passes through the target test position and is parallel to the Y-axis.

g is the deviation in mm along the g -axis from the exact position d and must be determined according to the procedure defined below. The g -axis is in the X-Z plane, passes through the target test position and is tangent to the conical section of the forearm phantom.

The e -axis is in the X-Z plane and is perpendicular to the f -axis and g -axis and is normal to the surface of the forearm phantom at the target test position.

r_1 , r_2 and r_3 are angular deviations in degrees around the e -axis, f -axis and g -axis respectively from the exact position and must be determined according to the procedure defined below.

$k_1 = 0.04$, $k_2 = 0.16$, $k_3 = 0.04$, $k_4 = 0.64$ and $k_5 = 0.10$ are the sensitivity factors which were determined according to the methodology outlined in Section 3. The maximum sensitivity has been expanded by the number of degrees of freedom. If the maximum deviations for f , g , r_1 , r_2 and r_3 are determined according to 2.13.2.5 Step 6, then a rectangular distribution (divisor = 1.73) shall be used. If f , g , r_1 , r_2 and r_3 are determined as standard deviations assuming a normal distribution. In this case, the standard deviation shall be treated as a standard uncertainty (divisor = 1) shall be used in Table 2.13.3.4-1. These equations are only valid for f and $g \leq 2$ mm, $r_1 \leq 5^\circ$, $r_2 \leq 2^\circ$ and $r_3 \leq 0.5^\circ$.

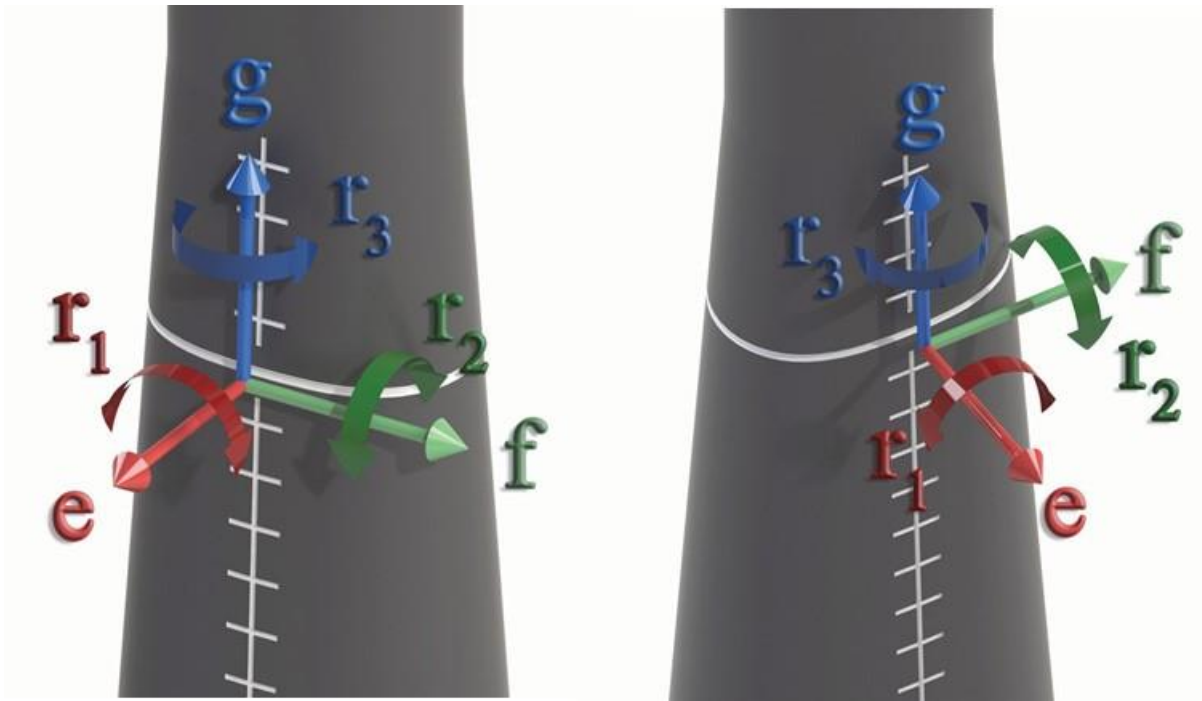


Figure 2.13.3.2-1 Forearm Positioning Uncertainty Components

2.13.3.3 Forearm Phantom Fixturing Requirements

The primary goal of the fixture is to allow the stable mounting of the forearm phantom and DUT in the chamber, while also being transparent and non-reflective to RF. The material for the forearm phantom fixturing shall have a dielectric constant of less than 5.0 and a loss tangent of less than 0.05. The fixturing shall be kept below the base of the forearm phantom.

No additional measurement uncertainty from the forearm phantom fixture is needed as long as the above requirements are met.

2.13.3.4 Example of Uncertainty for Reasonably Worst-case Forearm and DUT Positioning on Forearm (Informative)

The uncertainty for reasonably worst-case forearm and DUT positioning on forearm is provided in [Table 2.13.3.4-1](#).

Table 2.13.3.4-1 Example of Uncertainty Assessment for Reasonably Worst-Case Forearm and DUT Positioning on Forearm

Uncertainty Component	Tolerance/ Uncertainty Value (± dB)	Probability Distribution	Divisor	c _i	Standard Uncertainty (± dB)	v _i or v _{eff}
	a		b	c	U _i = (a/b) × (c)	
Forearm Phantom						
Material Dielectric Constant	0.59	Rectangular	1.73	0.71	0.24	
Material Conductivity	1.10	Rectangular	1.73	0.42	0.29	
Geometry/Shape (incl. spacer)	<0.1	Rectangular	1.73	0.00	0.00	
Combined Forearm Phantom Uncertainty					0.38	

Fixtures						
Forearm Phantom Fixture		Rectangular	1.73	0.00	0.00	
DUT Related						
DUT Positioning	0.37	Rectangular	1.73	1.00	0.21	
Combined Standard Uncertainty (Forearm)					0.43	

Forearm Phantom						
	$\Delta\epsilon_{avg}/\epsilon$	ϵ_{unc}/ϵ	ϵ_{std}/ϵ	a_1	a	
Material Dielectric Constant	0.1	0.03	0.2	0.5	0.59	Reference Equation 2.13.2.2-1
	$\Delta\sigma_{avg}/\sigma$	σ_{unc}/σ	σ_{std}/σ	a_1	a	
Material Conductivity	0.2	0.05	0.4	0.5	1.10	Reference Equation 2.13.2.2-2

DUT Related							
	g (mm)	f (mm)	r₁ (deg)	r₂ (deg)	r₃ (deg)	a	
DUT Positioning	1	1	2	0.5	0.5	0.37	Reference Equation 2.13.3.2-1

2.13.4 Uncertainties Related to Testing with Chest Phantom (Informative) SISO, Anechoic.

2.13.4.1 Uncertainty Related to Chest Phantom

This uncertainty shall be determined using the method described in Section 2.13.2.2 except that the method is applied to the chest phantom instead of a hand phantom.

When measuring the relative permittivity and conductivity, refer to Table 2.13.3.4-1 for the coordinates of twelve test locations defined for chest phantoms. Figure 2.13.4.1-1 highlights the test points on the phantom.

For the chest phantoms meeting the minimal requirements defined in Section 2.13.2.2, the approximations given in Equation 2.13.4.1-1 through Equation 2.13.4.1-3 shall be used to determine the chest uncertainty where a rectangular distribution is assumed. The constants, c_1 , c_2 and a_1 , as used in Equation 2.13.4.1-1 and Equation 2.13.4.1-2, were determined for chest phantoms according to the methodology outlined in Section 3 to be $c_1 = 0.46$, $c_2 = 0.30$ and $a_1 = 0.50$.

As used in Equation 2.13.4.1-3, $\Delta shape$ is the uncertainty on TRP, resulting from the tolerance of the chest phantom shape. Since the chests are usually manufactured with molds, the tolerance is 2% and therefore the effect is negligible, i.e., $c_3 = 0$. If the tolerance is larger, a numerical study as outlined in Section 3 must be conducted to determine $\Delta shape$.

The total standard uncertainty (root-sum-squares of $u_{chest_phantom_permittivity}$, $u_{chest_phantom_conductivity}$, $u_{chest_phantom_shape}$) shall not exceed 0.5 dB.

Equation 2.13.4.1-1

$$u_{chest_phantom_permittivity}[\text{dB}] = c_1 \cdot \left[10 \cdot \log_{10} \left(1 + \left| \frac{\sqrt{\Delta\varepsilon_{avg}^2 + \varepsilon_{unc}^2 + (a_1\varepsilon_{std})^2}}{\varepsilon} \right| \right) \right]$$

Equation 2.13.4.1-2

$$u_{chest_phantom_conductivity}[\text{dB}] = c_2 \cdot \left[10 \cdot \log_{10} \left(1 + \left| \frac{\sqrt{\Delta\sigma_{avg}^2 + \sigma_{unc}^2 + (a_1\sigma_{std})^2}}{\sigma} \right| \right) \right]$$

Equation 2.13.4.1-3

$$u_{chest_phantom_shape}[\text{dB}] = c_3 \cdot \left[10 \cdot \log_{10} \left(1 + \left| \frac{\Delta shape}{shape} \right| \right) \right]$$

whereby,

$\Delta\varepsilon_{avg}$, $\Delta\sigma_{avg}$, ε_{std} , σ_{std} are the values determined as defined above and ε_{unc} and σ_{unc} are expanded measurement uncertainties ($k = 2$) of the dielectric parameters according to Section 2.13.1 determined for homogeneous materials.

Table 2.13.4.1-1 Coordinates of Twelve Locations for Dielectric Measurements on the Chest Phantom

Point	X (mm)	Y (mm)	Z (mm)
P1	-70	20	0
P2	-20	20	0
P3	20	20	0
P4	70	20	0
P5	-70	-20	0
P6	-20	-20	0
P7	20	-20	0
P8	70	-20	0
P9	-50	-125	0
P10	50	-125	0
P11	-50	125	0
P12	50	125	0

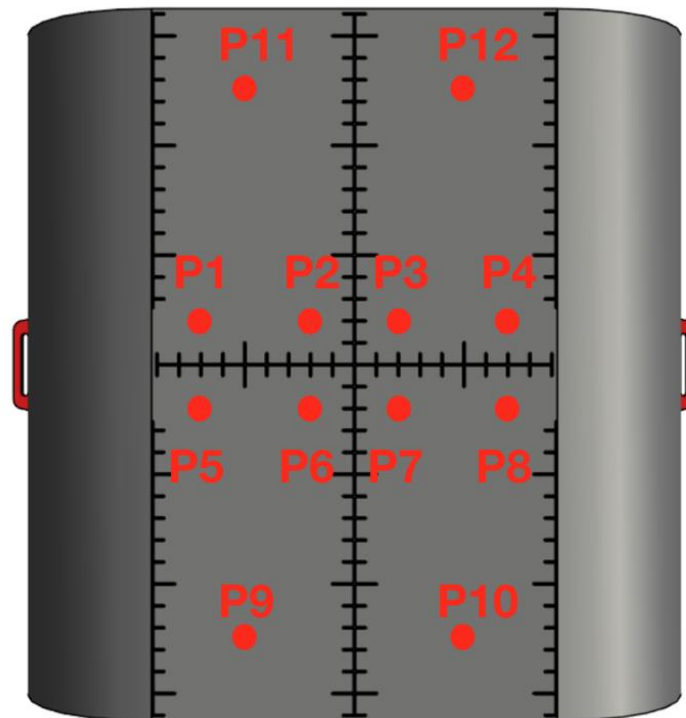


Figure 2.13.4.1-1 Twelve Locations for Dielectric Measurements on the Chest Phantom

2.13.4.2 Uncertainty Related to Chest-Worn Device Positioning

This uncertainty shall be determined using the method described in Section 2.13.2.5 except that the method is applied to the chest phantom instead of a hand phantom.

When recording the position of the DUT relative to the available reference marks on the chest phantom (Section 2.13.2.5, step 2), include position offsets in directions x and y and angular rotations r_1 , r_2 and r_3 shown in Figure 2.13.4.2-1.

A similar approximation to that given for hands phantoms (Equation 2.13.5.2-1) shall be used to determine the chest phantom positioning uncertainty:

Equation 2.13.4.2-1

$$u_{\text{positioning}}[\text{dB}] = \sqrt{(k_1 \cdot |f|)^2 + (k_2 \cdot |g|)^2 + (k_3 \cdot |r_1|)^2 + (k_4 \cdot |r_2|)^2 + (k_5 \cdot |r_3|)^2}$$

where: f is the deviation in the x direction (see Figure 2.13.4.2-1) in mm from the exact position described in Section 2.4 of CTIA 01.71 [4] and must be determined according to the procedure defined below.

g is the deviation in the y direction (see Figure 2.13.4.2-1) in mm from the exact position described in Section 2.4 of CTIA 01.71 [4] and must be determined according to the procedure defined below.

r_1 , r_2 and r_3 are angular deviations (see Figure 2.13.4.2-1) in degrees from the exact position described in Section 2.4 of CTIA 01.71 [4] and must be determined according to the procedure defined below. r_1 is the rotation around the z -axis, r_2 is the rotation around the y -axis and r_3 is the rotation around the x -axis.

$k_1 = 0.02$, $k_2 = 0.02$, $k_3 = 0.10$, $k_4 = 0.10$ and $k_5 = 0$ are the sensitivity factors which were determined according to the methodology outlined in Section 3. The maximum sensitivity has been expanded by the number of degrees of freedom. If the maximum deviations for f , g , r_1 , r_2 and r_3 are determined according to Section 2.13.2.5, Step 6, then a rectangular distribution (divisor = 1.73) shall

be used. If f, g, r_1, r_2 and r_3 are determined as standard deviations, then a normal distribution (divisor = 1) shall be used in [Table 2.13.4.3-1](#).

These equations are only valid for f and $g \leq 2 \text{ mm}$, $r_1 \leq 2^\circ$, $r_2 \leq 2^\circ$ and $r_3 \leq 5^\circ$.

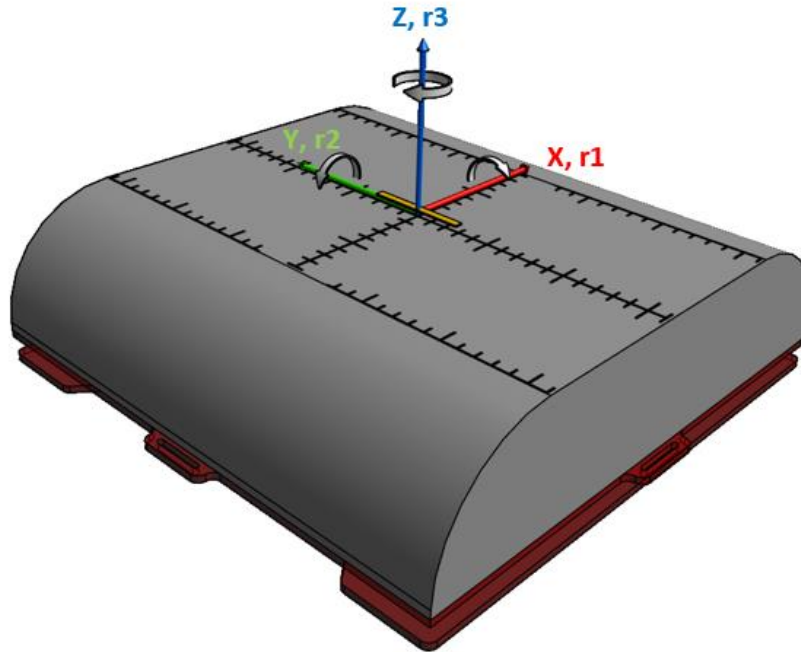


Figure 2.13.4.2-1 Chest Positioning Uncertainty Components

2.13.4.3 Example of Uncertainty for Reasonably Worst-Case Chest and DUT Positioning on Chest (Informative)

The uncertainty for reasonably worst-case chest and DUT positioning on chest is provided in [Table 2.13.4.3-1](#).

Table 2.13.4.3-1 Example of Uncertainty Assessment for Reasonably Worst-case Chest and DUT Positioning on Chest

Uncertainty Component	Tolerance/ Uncertainty Value (± dB)	Probability Distribution	Divisor	c_i	Standard Uncertainty (± dB)	v_i or v_{eff}
	a		b	c		
Chest Phantom						
Material Dielectric Constant	0.59	Rectangular	1.73	0.46	0.16	
Material Conductivity	1.10	Rectangular	1.73	0.30	0.19	
Geometry/Shape (incl. spacer)	< 0.1	Rectangular	1.73	0.00	0.00	
Combined Chest Phantom Uncertainty					0.25	
Fixtures						

Chest Phantom Fixture		Rectangular	1.73	0.00	0.00	
DUT Related						
DUT Positioning	0.21	Rectangular	1.73	1	0.12	
Combined Standard Uncertainty (Chest)					0.28	

Chest Phantom						
	$\Delta\varepsilon_{avg}/\varepsilon$	$\varepsilon_{unc}/\varepsilon$	$\varepsilon_{std}/\varepsilon$	a_1	a	
Material Dielectric Constant	0.1	0.03	0.20	0.5	0.59	Reference Equation 2.13.2.2-1
	$\Delta\sigma_{avg}/\sigma$	σ_{unc}/σ	σ_{std}/σ	a_1	a	
Material Conductivity	0.2	0.05	0.4	0.50	1.10	Reference Equation 2.13.2.2-2

DUT Related							
	g (mm)	f (mm)	r_1 (deg)	r_2 (deg)	r_3 (deg)	a	
DUT Positioning	1	1	2	0.5	0.5	0.21	Reference Equation 2.13.4.2-1

2.13.5 Uncertainties Related to Testing with Ankle Phantom (Informative) SISO, Anechoic

2.13.5.1 Ankle Phantom Uncertainty

This uncertainty shall be determined using the method described in Section 2.13.2.2 except that the method is applied to the ankle phantom instead of a hand phantom.

When measuring the relative permittivity and conductivity, refer to Table 2.13.5.1-1 for the coordinates of twelve test locations defined for ankle phantoms. Figure 2.13.5.1-1 highlights the test points on each face of the phantom.

For the ankle phantoms meeting the minimal requirements defined in Section 2.13.2.2, the approximations given in Equation 2.13.5.1-1 through Equation 2.13.5.1-3 shall be used to determine the ankle uncertainty where a rectangular distribution is assumed. The constants, c_1 , c_2 and a_1 , as used in Equation 2.13.5.1-1 and Equation 2.13.5.1-2 were determined for ankle phantoms according to the methodology of Section 3 to be $c_1 = 0.24$, $c_2 = 0.22$ and $a_1 = 0.50$.

As used in Equation 2.13.5.1-3, $\Delta shape$ is the uncertainty on TRP, resulting from the tolerance of the ankle phantom shape. Since the ankles are usually manufactured with molds, the tolerance is 2% and therefore the effect is negligible, i.e., $c_3 = 0$. If the tolerance is larger, a numerical study as outlined in Section 3 must be conducted to determine $\Delta shape$.

The total standard uncertainty (root-sum-squares of $U_{ankle_phantom_permittivity}$, $U_{ankle_phantom_conductivity}$, $U_{ankle_phantom_shape}$) shall not exceed 0.5 dB.

Equation 2.13.5.1-1

$$u_{ankle_phantom_permittivity}[\text{dB}] = c_1 \cdot \left[10 \cdot \log_{10} \left(1 + \left| \frac{\sqrt{\Delta\varepsilon_{avg}^2 + \varepsilon_{unc}^2 + (a_1\varepsilon_{std})^2}}{\varepsilon} \right| \right) \right]$$

Equation 2.13.5.1-2

$$u_{ankle_phantom_conductivity}[\text{dB}] = c_2 \cdot \left[10 \cdot \log_{10} \left(1 + \left| \frac{\sqrt{\Delta\sigma_{avg}^2 + \sigma_{unc}^2 + (a_1\sigma_{std})^2}}{\sigma} \right| \right) \right]$$

Equation 2.13.5.1-3

$$u_{ankle_phantom_shape}[\text{dB}] = c_3 \cdot \left[10 \cdot \log_{10} \left(1 + \left| \frac{\Delta shape}{shape} \right| \right) \right]$$

whereby,

$\Delta\varepsilon_{avg}$, $\Delta\sigma_{avg}$, ε_{std} , σ_{std} are the values determined as defined above and ε_{unc} and σ_{unc} are expanded measurement uncertainties ($k = 2$) of the dielectric parameters according to Section 2.13.1 determined for homogeneous materials.

Table 2.13.5.1-1 Coordinates of Twelve Locations for Dielectric Measurements on the Ankle Phantom

Point	X (mm)	Y (mm)	Z (mm)
P1	Outer Side	-20	20
P2	Outer Side	-20	-20
P3	Outer Side	20	20
P4	Outer Side	20	-20
P5	Outer Side	-20	170
P6	Inner Side	20	20
P7	Inner Side	20	-20
P8	Inner Side	-20	20
P9	Inner Side	-20	-20
P10	Inner Side	20	170
P11	15	-100	Sole of the Foot
P12	15	-100	Top of the Foot

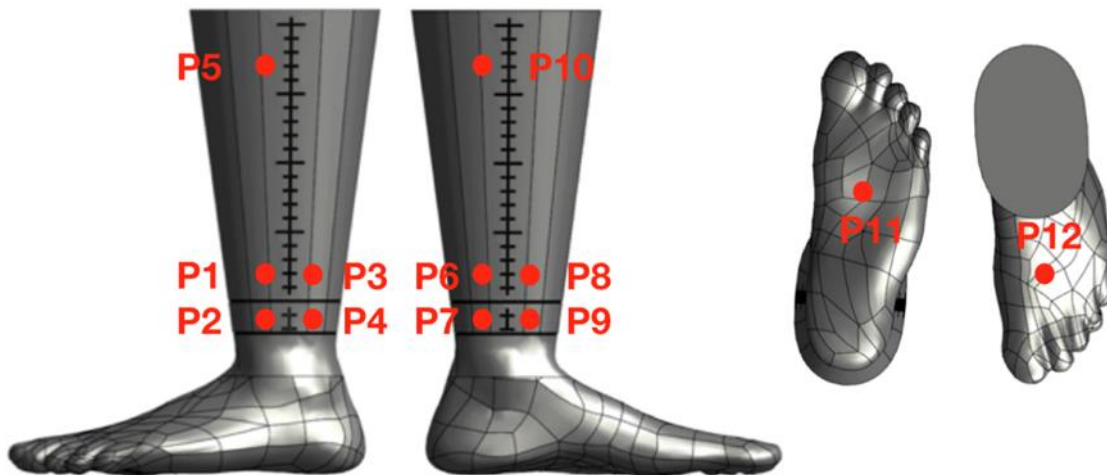


Figure 2.13.5.1-1 Twelve Locations for Dielectric Measurements on the Ankle Phantom

2.13.5.2 Ankle-Worn Device Positioning Uncertainty

This uncertainty shall be determined using the method described in Section 2.13.2.5 except that the method is applied to the ankle phantom instead of a hand phantom.

When recording the position of the DUT relative to the available reference marks on the ankle phantom (Section 2.13.2.5, step 2), include position offsets in directions g and f and angular rotations r_1 , r_2 and r_3 shown in Figure 2.13.5.2-1.

A similar approximation to that given for hands phantoms (Equation 2.13.2.5.2-1) shall be used to determine the ankle phantom positioning uncertainty:

Equation 2.13.5.2-1

$$u_{\text{positioning}} [\text{dB}] = \sqrt{(k_1 \cdot |f|) + (k_2 \cdot |g|) + (k_3 \cdot |r_1|) + (k_4 \cdot |r_2|) + (k_5 \cdot r_3)}$$

where: f is the deviation in the x direction (see Figure 2.13.5.2-1) in mm from the exact position described in CTIA 01.71 [4] Section 2.5 and must be determined according to the procedure defined below.

g is the deviation in the y direction (see Figure 2.13.5.2-1) in mm from the exact position described in CTIA 01.71 [4] and must be determined according to the procedure defined below.

r_1 , r_2 and r_3 are angular deviations (see Figure 2.13.5.2-1) in degrees from the exact position described in CTIA 01.71 [4] Section 2.5 and must be determined according to the procedure defined below. r_1 is the rotation around the z -axis, r_2 is the rotation around the y -axis and r_3 is the rotation around the x -axis.

$k_1 = 0.04$, $k_2 = 0.20$, $k_3 = 0.02$, $k_4 = 0.17$ and $k_5 = 0.03$ are the sensitivity factors which were determined according to the methodology of Section 3. The maximum sensitivity has been expanded by the number of degrees of freedom. If the maximum deviations for f , g , r_1 , r_2 and r_3 are determined according to Section 2.13.2.5, Step 6, then a rectangular distribution (divisor = 1.73) shall be used. If f , g , r_1 , r_2 and r_3 are determined as standard deviations, then a normal distribution (divisor = 1) shall be used in Table 2.13.5.3-1.

These equations are only valid for f and $g \leq 2 \text{ mm}$, $r_1 \leq 5 \text{ degrees}$, $r_2 \leq 0.5 \text{ degrees}$ and $r_3 \leq 2 \text{ degrees}$.

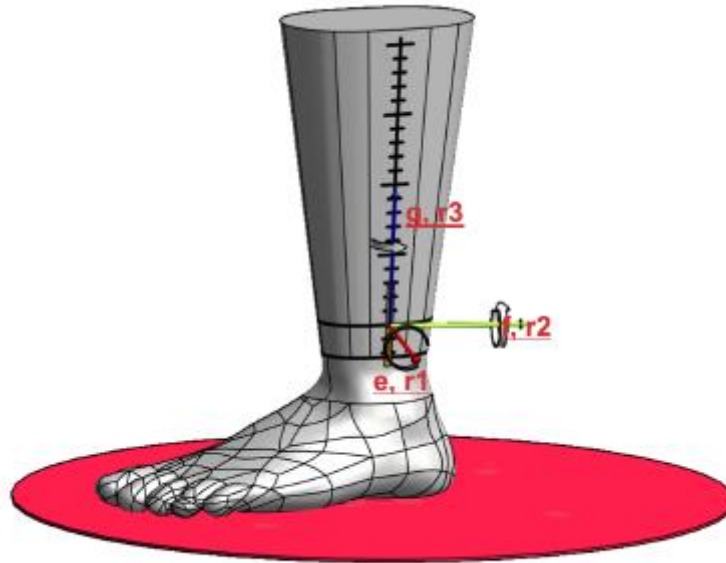


Figure 2.13.5.2-1 Ankle Positioning Uncertainty Components

2.13.5.3 Uncertainty for Reasonably Worst-Case Ankle and DUT Positioning on Ankle

The uncertainty for reasonably worst-case ankle and DUT positioning on ankle is provided in [Table 2.13.5.3-1](#).

Table 2.13.5.3-1 Example of Uncertainty Assessment for Reasonably Worst-case Ankle and DUT Positioning on Ankle

Uncertainty Component	Tolerance/ Uncertainty Value (\pm dB)	Probability Distribution	Divisor	c_i	Standard Uncertainty (\pm dB)	v_i or v_{eff}
	a		b	c		
Ankle Phantom						
Material Dielectric Constant	0.59	Rectangular	1.73	0.24	0.08	
Material Conductivity	1.10	Rectangular	1.73	0.22	0.14	
Geometry/Shape (incl. spacer)	<0.1	Rectangular	1.73	0.00	0.00	
Combined Ankle Phantom Uncertainty					0.17	
Fixtures						
Ankle Phantom Fixture		Rectangular	1.73	0.00	0.00	
DUT Related						
DUT Positioning	0.21	Rectangular	1.73	1	0.12	

Combined Standard Uncertainty (Ankle)		0.21	
---------------------------------------	--	------	--

Ankle Phantom						
	$\Delta\epsilon_{avg}/\epsilon$	ϵ_{unc}/ϵ	ϵ_{std}/ϵ	a_1	a	
Material Dielectric Constant	0.10	0.03	0.20	0.50	0.59	Reference Equation 2.13.2.2-1
	$\Delta\sigma_{avg}/\sigma$	σ_{unc}/σ	σ_{std}/σ	a_1	a	
Material Conductivity	0.20	0.05	0.40	0.50	1.10	Reference Equation 2.13.2.2-2

DUT Related							
	g (mm)	f (mm)	r_1 (deg)	r_2 (deg)	r_3 (deg)	a	
DUT Positioning	1	1	2	0.5	0.5	0.21	Reference Equation 2.13.5.2-1

2.14 Positioning Misalignment

This contribution originates from the misalignment of the test direction and the beam peak direction of the measurement antenna due to imperfect rotation operation. The pointing misalignment may happen in both azimuth and elevation directions and the effect of the misalignment depends highly on the beam width of the beam under test. The same level of misalignment results in a larger measurement error for a narrower beam.

2.15 Misalignment of Positioning System

This contribution originates from uncertainty in sliding position and turn table angle/tilt accuracy. If the calibration antenna is aligned to the beam peak this contribution can be considered negligible and therefore set to zero.

2.16 Positioning and Pointing Misalignment between the Reference Antenna and the Measurement Antenna

This contribution originates from reference antenna alignment and pointing error. In this measurement if the maximum gain direction of the reference antenna and the transmitting antenna are aligned to each other, this contribution can be considered negligible and therefore set to zero.

2.17 DUT Positioning/Repositioning Uncertainty

Free-space testing and multi-step test processes such as RSS based TIS and the various alternate test methods require one or more positioning uncertainty contribution(s).

For free-space testing, the orientation of the DUT in the mounting fixture can have small effects on the overall TRP/TIS and near horizon numbers due to slight differences in alignment. In addition, any near field interactions with the dielectric support can have an effect. Repeated TRP tests of a sample device with minor mounting changes between each test can be used to estimate this effect.

For RSS and alternate methods that rely on single point normalization techniques, any difference in the position between reference and target measurements can change the relative results and produces a repositioning error that may just be the result of automated positioning. Since this is a pattern related result instead of an average result like TRP/TIS, the variation at the peak of the DUT pattern can be used to estimate this quantity. For the purposes of this contribution, interpolated TRP pattern data can be used to determine the maximum change expected due to a one-degree positioning change. This term shall be treated as a rectangular distribution.

In cases where the DUT is repositioned relative to the head/hand/fixture (e.g., due to lost call or battery change) between steps of a relative test, the appropriate positioning uncertainty shall be applied a second time as a repositioning uncertainty.

2.18 DUT Repositioning

This contributor describes the uncertainty due to a misalignment of a DUT. The DUT may need to be re-oriented to avoid forming its beam toward the support structure during the measurement or when the device is placed back into the support structure after battery ran low in charge.

2.19 Measurement Setup Repeatability

Select a representative device and repeat the corresponding measurement 10 times, unmounting and remounting the DUT and DUT fixture for each measurement. Calculate the standard deviation of the metric obtained and use that as the measurement uncertainty. For tests that require multiple setups (i.e. Portrait and Landscape), the worst-case standard deviation shall be used.

2.20 Receiver Performance Search Step Size

The step size of the power level used in the measurement must be evaluated as an uncertainty contribution.

There are two possible approaches for the downlink power uncertainty term. The lab shall indicate which approach was used to evaluate the uncertainty term.

2.20.1 Fixed Step Size without Interpolation

The power uncertainty term can be evaluated as a fixed step size. Excluding other uncertainty contributions, the actual threshold power level ranges from the reported level to one step below the reported level. This can be represented as an asymmetric uncertainty contribution of +0/-step size, with a rectangular distribution. However, on average, the actual threshold, and thus the resulting threshold level, will be one-half step below the reported value. For the purposes of this test plan, this uncertainty contribution is assumed to be symmetrical with a fixed uncertainty contribution of \pm one-half of the step size.

For the TIS measurement grids outlined in Table 4.1-1 of *CTIA 01.20* [5], the step sizes and standard uncertainty contributions (actual distribution) listed in [Table 2.20.1-1](#) should be reported for the step size uncertainty. For other measurement grids, see Section [2.21.2](#).

Table 2.20.1-2: Uncertainty Contributions and Step Sizes

Applicability Condition	$\Delta\theta = \Delta\phi$ [°]	Step Size [dB]	Standard Uncertainty Contribution [dB]
Below 3 GHz and Device Size \leq 30 cm	45	0.25	0.11
Below 3 GHz and Device Size $>$ 30 cm	30	0.5	0.14
Above 3 GHz	30	0.5	0.14

2.20.2 Fixed Step Size with Interpolation

This approach performs the leveling with power steps but calculates the power level required for obtaining a nominal throughput threshold by interpolating on a curve of measurement points. This approach is preferred since it reduces the uncertainty even further.

The resulting uncertainty term must be evaluated from the typical smoothness of the curve and the spacing of its points. Guidance for a quantitative estimate of the uncertainty comes from the solution providers.

2.21 Grid Related Measurement Uncertainty

2.21.1 Coarse Sampling Grid for TIS Measurements below 6 GHz

The sampling grids for TIS measurements are outlined in Table 4.1-1 of *CTIA 01.20* [5]. The uncertainty arises from an assessment of how different the results for this spacing would be from an infinitely small sampling grid. It is possible to argue that, since all test houses are required to measure at the same 30° grid points using the same coordinate axes, all results would have the same value of uncertainty. However, this is not an adequate assessment since some carriers will be basing acceptance of handsets on the assumption that the measured values are correct; we need therefore to include, as an uncertainty, the contribution of this effect.

The fixed standard uncertainty values for the TIS measurement grids outlined in Table 4.1-1 of *CTIA 01.20* [5] that shall be reported are listed in Table 2.21.1-1.

Table 2.21.1-1: Uncertainty Contributions and Step Sizes

Applicability Condition	$\Delta\theta$ [°]	Standard Uncertainty Contribution [dB]
Below 3 GHz and Device Size \leq 30 cm	45	0.11
Below 3 GHz and Device Size $>$ 30 cm	30	0.23
Above 3 GHz	30	0.23

Note: The uncertainty distribution shall be assumed to be actual

Note: The sampling grids used in TRP tests are assumed to produce negligible uncertainty. See Table 3.1-1 in *CTIA 1.20* [5] for applicabilities.

2.21.2 Reduction in the Number of Test Samples on TIS Measurements below 6 GHz

It has been proven elsewhere that the numerical effect of the theta dependent phi optimization on the resultant pattern is negligible. However, for TIS, the reduction in the number of EIS points that are averaged into the resultant TIS can have an impact on the resulting TIS value. The current uncertainty budget does not independently isolate the random error of a single EIS measurement, so for the purpose of this discussion we will assume that the average of that random error is encapsulated in the Sensitivity Search Step Size uncertainty term defined in Section 2.20.

In general, the average of N repeat measurements containing a random uncertainty term, u_c , will reduce the corresponding random uncertainty by a factor of $1/\sqrt{N}$. Thus, reducing the number of data points for a given cut from N to M will increase the random uncertainty of that cut by the factor of $\sqrt{N/M}$. However, since each cut is weighted by the Clenshaw-Curtis weight, the corresponding error contribution from that cut in the resulting TIS is also reduced by the same amount in linear units.

Rather than attempting to account for the spherical weighting of each curve, the assumption here will be that the total step size uncertainty increases by a factor of $\sqrt{N/M}$. The standard uncertainty contribution shall be reported respective step sizes and number of grid points M .

Table 2.21.2-1: Standard Uncertainty for TIS measurement grids

Step Size [dB]	Uncertainty with rectangular distribution [dB]	Std. Uncertainty Contribution for 62 points [dB]	N	M	Measurement Grid Type	$\Delta\theta$ [°]	Std. Uncertainty Contribution for M points [dB]
0.5	0.25	0.14	62	62	Constant Angular Step Size	30	0.14
0.5	0.25	0.14	62	46	Theta Dependent Phi Optimization	30	0.17
0.25	0.125	0.07	62	26	Constant Angular Step Size	45	0.11
0.25	0.125	0.07	62	20	Theta Dependent Phi Optimization	45	0.13

2.21.3 Influence of Millimeter Wave TRP Measurement Grid

This contributor describes the uncertainty of the measured TRP value due to the finite number of measurement grid points. See Section 8.1 in *CTIA 01.22* [7] for more details.

2.21.4 Influence of Millimeter Wave Spherical Coverage Grid

This contributor describes the uncertainty of spherical measurements, due to the finite number of measurement points in the spherical coverage grid. See Section 8.3 of *CTIA 01.22* [7] for more details.

2.22 Miscellaneous Uncertainty

In this test plan, the term 'miscellaneous uncertainty' is used to account for all the unknown, unquantifiable, etc. uncertainties associated with the measurements. This term includes truly random effects as well as systematic uncertainties, such as that arising from dissimilarity between the patterns of the reference antenna and the DUT. The random uncertainty term, by definition, cannot be measured, or even isolated completely.

This term includes, but is not limited to, the following effects:

- Pattern difference effect
- Humidity effects
- Temperature effects (not so much on equipment or the DUT - more on the losses of cables, attenuators, etc.)
- Personnel
- Dirty connector interfaces

This contribution shall be accounted for using a fixed value of 0.5 dB for millimeter wave bands or 0.2 dB below 6 GHz and a normal distribution (i.e. standard uncertainty = 0.25 dB or 0.1 dB). For millimeter wave bands the value of 0.5 dB is chosen due to the increased sensitivity to random effects in more complex, higher frequency test systems.

If a lab is aware of any significant uncertainty terms not included in this test plan, they shall be included in the lab's uncertainty budget and reported.

2.23 TIS Normalization Uncertainty

This uncertainty component arises when using the single point or multi-point alternate test method for TIS testing as described in *CTIA 01.20* [5].

Using the nomenclature of this document, test configuration A will be the protocol/error rate/data rate for which a full TIS measurement is performed while test configuration B will be the target protocol/error rate/ data rate which will be tested using the single/multi-point radiated test.

The normalization uncertainty shall be treated as follows.

1. Calculate the standard uncertainty associated with the test configuration A measurement (as used for the full TIS measurement) by dividing half of the step size by $\sqrt{3}$ and by the square root of the number of measurements at different spatial positions which are averaged.

$$u_{j A} = \frac{\text{Step Size}_A}{2\sqrt{3} * \text{Number of Measurements}}$$

2. Calculate the standard uncertainty associated with the test configuration B measurement (a single or multi-point measurement) by dividing half of the step size by $\sqrt{3}$ and by the square root of the number of measurements at different spatial positions which are averaged.

$$u_{j B} = \frac{\text{Step Size}_B}{2\sqrt{3} * \text{Number of Measurements}}$$

3. Combine both of the uncertainty quantities with the other uncertainty contributions by root-sum-squares.

2.24 Linearization of RSS Measurements

This uncertainty component arises from linearizing the conducted or radiated RSS measurements. The uncertainty is defined as the maximum standard deviation of the raw conducted or radiated RSS data from the final normalized conducted or radiated RSS data.

It is the responsibility of the lab to measure the maximum standard deviation, and this needs to be converted to dB, if necessary.

2.25 Uncertainty of RSS Data from DUT

This uncertainty component refers to the integrity of the data reported, or recorded, by the DUT.

- The RSS measurements reported by the DUT shall be verified by examining the variance of the data in real time to ensure that it is not skewed by an erroneous reading. This variance check shall be used to determine if a data point requires retesting.

OR

- The RSS measurements recorded by the DUT shall be verified using a post processing variance check to ensure that the data is not skewed by an erroneous reading. This variance check shall be used to determine if a data point requires retesting.

It is the responsibility of the lab to determine the maximum variance of the data obtained from the DUT and this will need to be converted to dB, if necessary.

Note: This uncertainty term may be combined with the Section 2.13 uncertainty term and reported as one uncertainty term.

2.26 Reporting Mechanism for RSS Data from EU

When the DUT either reports, or records, the RSS data at each position on the 3-D measurement sphere, there is an uncertainty introduced by this reporting mechanism that is inherent to the DUT. This uncertainty contribution refers to the quantization error present in the RSS data reported, or recorded, by the DUT at each data point on the 3-D measurement sphere.

It is the responsibility of the lab to determine the maximum quantization error of the data obtained from the DUT and this will need to be converted to dB, if necessary. This uncertainty term shall be assumed to be rectangularly distributed, in which case the standard uncertainty shall be calculated as:

$$\frac{\text{maximum value}}{\sqrt{3}}$$

2.27 Uncertainty Due to Difference in Gain Over Different Channel Bandwidths

For relative measurements of different protocols with different channel bandwidths, there may be a difference in the associated path loss.

A conservative way of assessing the uncertainty due to the difference in system path loss over the different channel bandwidths is to perform the following steps:

1. Estimate the system path loss as a function of frequency by applying an appropriate curve fit to the measured system path loss.
2. Calculate the average system path loss over each channel bandwidth.

$$\overline{PL}(a, b) = \frac{1}{b - a} \int_a^b PL(f) df$$

$\overline{PL}(a, b)$ = average path loss over the frequency interval a to b

$PL(f)$ = path loss as a function of frequency

3. The measurement uncertainty is then the difference in average system path loss over the 2 different channel bandwidths.

For systems with path loss variation less than 3 dB over a 25 MHz band containing the channel bandwidths of interest, a fixed uncertainty contribution of 0.2 dB with a rectangular distribution (standard uncertainty of 0.115 dB) may be used.

2.28 Test System Frequency Flatness Uncertainty

For wireless technologies with channel bandwidths more than 2 MHz, there is a likelihood that the test system used will not have a flat frequency response across the entire channel. While the range calibration corrects for any variation of frequency response as a function of the center frequency of the channel, the broadband power measured from one of these technologies will be a function of the entire channel bandwidth as opposed to just the center frequency. Thus, any deviation of the rest of the channel from the signal level at the center frequency will result in an error in the measured result. For average power measurements, the error may be measured and corrected for, thereby minimizing the impact on measurement uncertainty. Where error correction is not possible or practical, the lab shall account for the total measurement uncertainty due to channel frequency response variation. Even with average channel power error correction, there may still be small uncertainty contributions related to frequency interpolation error that may need to be addressed. In addition, sensitivity measurement results are not necessarily a linear function of average channel power, resulting in some additional measurement uncertainty bias.

To determine the appropriate error correction or measurement uncertainty for total channel power, use range calibration curves measured with a frequency resolution sufficient to produce smoothly varying

frequency response curves with no evidence of higher order contributions. While resolutions on the order of 1 MHz are likely to be sufficient for most systems, resolutions closer to the channel or RB allocation resolution (e.g. ~200 kHz) are recommended to minimize interpolation error. After applying the reference antenna gain, convert the path loss data to linear power units then perform a running average across the band, averaging the data points across the corresponding channel bandwidth. The following equation describes the expected error contribution that this uncertainty must address:

Equation 2.28-1

$$\varepsilon_j = 10 \log \left(\frac{\sum_{k=j-N/2}^{j+N/2} PL_k}{(N+1)PL_j} \right)$$

where ε_j is the expected relative error in the average power result for a given channel in dB, PL_j , is the linear path loss at the center frequency of the given channel, PL_k , is the linear path loss at each frequency point across the corresponding channel, and N is the number of frequency steps across a given channel bandwidth. Note that $N+1$ points are actually averaged together from one edge of the channel to the other. This error may be removed directly at each frequency, f_j , by using the average path loss across the channel as the range loss correction rather than the path loss at the center frequency:

Equation 2.28-2

$$\overline{PL}_j(\text{dB}) = 10 \log \left(\frac{1}{N+1} \sum_{k=j-N/2}^{j+N/2} PL_k \right)$$

If not correcting for the average power error, the maximum deviation across all of the possible channels in a band shall be used to estimate the required channel flatness uncertainty contribution using a rectangular distribution so that:

$$u_i = a_i / \sqrt{3}, \text{ where } a_i \text{ is given by } a_i = \max(|\varepsilon_j|)$$

Assuming the frequency response is not under-sampled, the worst case error due to interpolation may be estimated as the maximum change in path loss magnitude between any two points within a band.

Equation 2.28-3

$$\varepsilon_{interpolation}(\text{dB}) = \max(|PL_{j+1}(\text{dB}) - PL_j(\text{dB})|)$$

This error shall be converted to an appropriate measurement uncertainty contribution using a rectangular distribution so that:

Equation 2.28-4

$$u_i = \varepsilon_{interpolation} / \sqrt{3}$$

Note that while sensitivity results may be more directly affected by the frequency dependent behavior of variations in channel flatness, such that the sensitivity result would be biased to a higher power level (worse sensitivity result), for the purposes of this test plan, this effect is deemed to be encompassed by the sensitivity search step size contribution in Section 2.20.

2.29 Frequency Flatness for TIS Measurements

For receiver sensitivity tests, where the receiver attempts to compensate for the frequency dependence of the channel, there is the potential for narrowband nulls in the frequency response of the channel to impact the error rate or throughput, thereby biasing the result away from that of a flat

channel with the same average power. While the net impact may be reduced through the use of wider coherence bandwidths and averaging across multiple stirrer samples, many of which may be flatter, any residual net bias would result in an error in the reported receiver sensitivity. Likewise, a bias in the estimate of the Reference may occur with an insufficient amount of loading or frequency averaging. This bias may increase for narrowband measurements. These errors and the associated measurement uncertainty are for future study.

2.30 Uncertainty Due to Implementation of Mode-Stirring Sequence and Chamber Lack of Spatial Uniformity

This component embodies the non-ideal effects of, for example, loading by the DUT or other components, a nonzero K factor and the limited number of modes within the chamber. This component reflects the uncertainty in positioning of the DUT and the reference antenna.

This component of uncertainty is determined by repeated reference measurements performed during a pre-characterization step, as described in *CTIA 01.21 [16]*. This uncertainty contribution is a composite value consisting of most of the specific reverberation chamber contributions, such as lack of spatial uniformity due to loading with RF absorber, limited number of modes, K-factor, and mode-stirring methods.

Note that both the number of mode-stirring samples and the variation in the estimate of G_{ref} due to lack of spatial uniformity will affect the value of $\sigma_{G_{\text{ref}}}$. Based on a significance test (see *CTIA 01.21 [16]*), it was determined that the variation due to lack of spatial uniformity was typically the dominant component of uncertainty in an estimate of G_{ref} because of the large number of mode-stirring samples that are generally used.

The standard uncertainty $u_{G_{\text{ref}}}$ for the reference and DUT measurement shall be calculated as:

Equation 2.30-1

$$u_{G_{\text{ref}},\text{nominal}} = \frac{\sigma_{G_{\text{ref}}}^i}{\sqrt{T_{\text{cal}}}}$$

where $\sigma_{G_{\text{ref}}}^i$ shall be found for the loading condition used in the DUT measurement from the table compiled in Section 6.2.3 in *CTIA 01.73 [2]*.

To compute the combined uncertainty as described in Section 3 of *CTIA 01.21 [16]*, a coverage factor of 2 will be applied. Because the uncertainty due to lack of spatial uniformity is computed from a limited number of samples ($T_{\text{pre}} = 12$), the coverage factor should be higher than 2 for this component of uncertainty. K_p is used to ensure that the expanded uncertainty will cover the expected 95% confidence. For this case, (11 degrees of freedom), the 95% coverage factor would be 2.201. Thus, the value of $K_p = 1.10$ is used to account for the limited number of samples for this element, resulting in the following expression to be used in the calculation of combined uncertainty:

Equation 2.30-2

$$u_{G_{\text{ref}}} = \frac{\sigma_{G_{\text{ref}}}^i}{\sqrt{T_{\text{cal}}}} \times K_p$$

Note that T_{cal} may be different for the reference and DUT measurements. For the reference measurements the value of T_{cal} is the number of positions/orientations used for the reverberation chamber calibration ($T_{\text{cal}} \geq 1$), and for the DUT measurement $T_{\text{cal}} = 1$.

The standard measurement uncertainty estimate shall be obtained for each channel bandwidth case as defined in *CTIA 01.21 [16]* by selecting the worst case for all available frequencies across each band. The value used for T_{cal} shall be reported in the MU budget and in the test report, in *CTIA 01.03 [17]*. Use separate MU templates for each channel bandwidth if necessary.

2.31 Chamber Standing Wave

This term accounts for a standing wave reflection between the measurement antenna and the DUT, representing an additional chamber ripple term beyond that recorded in the Quality of Quiet Zone validation. One method to obtain this value is to slide the DUT $\lambda/4$ towards the measurement antenna while measuring the amplitude. The uncertainty term can be derived by performing the standard deviation on the results. For more information, see Section 2.9.3.2.

For the IFF methodology, the chamber standing wave assessment in Section 2.9.3.2 is not applicable and the MU contribution is generally negligible.

2.32 Standing Wave between Reference Calibration Antenna and Measurement Antenna

This term comes from the amplitude ripple caused by the standing waves between the reference antenna and measurement antenna. This value can be captured by sliding ($\lambda/4$) the reference antenna towards the measurement antenna as the standing waves go in and out of phase causing a ripple in amplitude. The uncertainty term can be derived by performing the standard deviation on the results.

2.33 Phase Curvature

This contribution originates from the finite far field measurement distance, which causes phase curvature across the antenna under test (DUT or reference antenna). At a measurement distance of $2D^2/\lambda$ the phase curvature is 22.5° .

For large DUTs, the effect of phase curvature across the DUT on the integrated measurements of TRP and TIS is very small. Although the DUT may be relatively large, the actual antenna is small, and the phase curvature across the actual antenna will be insignificant. As a result, no additional uncertainty is required beyond that detailed in Section 2.9.

2.34 Influence of the XPD

This uncertainty is related to the measurement probe's polarization impurity, i.e., the propagation induced coupling of field components from the intended polarization into the un-intended cross-polarization and vice versa. The associated measurement uncertainty can be determined using the XPD (cross polarization discrimination) of the measurement probe.

A typical probe antenna can have XPD of 30 dB.

A transmission matrix and calibration setup as shown in Figure 2.34 1 is considered here. Typically, a single-polarized reference antenna with known gain is placed at the center of the quiet zone and the total attenuation, L , between the reference antenna terminal and the feed antenna terminals is determined as part of the range reference calibration procedure.

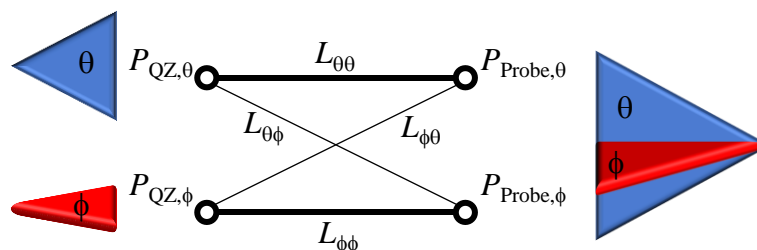


Figure 2.34-1 Calibration Setup

Since the reference antenna is considered a single-polarized antenna, the XPD effect is negligible. Since the measurement probe is assumed to be a dual-linearly polarized antenna, leakage from one terminal/polarization to the other, i.e., XPD, needs to be considered.

The dual-linearly polarized measurement probe has two terminals corresponding to a set of orthogonal polarizations, θ and ϕ which match the orientations of the reference antenna. The most thorough calibration procedure would determine the path losses between the four different combinations of signal paths: $\theta\theta$, $\theta\phi$, $\phi\theta$, and $\phi\phi$, e.g., the power received by the measurement probe at the θ polarization/terminal, $P_{Feed,\theta}$, is attenuated by $L_{\phi\theta}$ with respect to the power delivered to the reference antenna oriented in the ϕ polarization and placed in the center of quiet zone, $P_{QZ,\theta}$.

The most common calibration approach, however, is based on calibrating the polarization matched paths in Figure 2.34 1 (thick solid lines), i.e., $\theta\theta$ and $\phi\phi$. In this case, as illustrated in Figure 2.34 2 the normalized pathlosses $L_{\theta\theta}$ and $L_{\phi\phi}$ are 1 and the pathlosses of the crossed components become the XPD terms of the measurement probe:

Equation 2.34-1

$$\alpha_{\theta\phi} = 10^{\frac{XPD_{\theta\phi}}{10}}$$

and

Equation 2.34-2

$$\alpha_{\phi\theta} = 10^{\frac{XPD_{\phi\theta}}{10}}$$

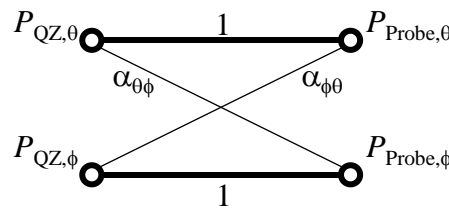


Figure 2.34-2 Common Calibration approach based on Calibrating the Polarization Matched Signal Paths

In the remainder of this analysis, it is assumed that the leakage between the two polarization ports of the measurement probe is assumed to be the same, i.e., $XPD = XPD_{\theta\phi} = XPD_{\phi\theta}$ and $\alpha = \alpha_{\theta\phi} = \alpha_{\phi\theta}$.

The normalized powers at the measurement probe terminals can then be written as:

Equation 2.34-3

$$P_{Probe,\theta} = P_{QZ,\theta} + \alpha P_{QZ,\phi}$$

Equation 2.34-4

$$P_{Probe,\phi} = P_{QZ,\phi} + \alpha P_{QZ,\theta}$$

The normalized ratio of total powers at measurement probe and the center of the quiet zone is therefore:

Equation 2.34-5

$$\frac{P_{Probe}}{P_{QZ}} = \frac{P_{Probe,\theta} + P_{Probe,\phi}}{P_{QZ,\theta} + P_{QZ,\phi}} = \frac{(P_{QZ,\theta} + P_{QZ,\phi})(1 + \alpha)}{P_{QZ,\theta} + P_{QZ,\phi}} = 1 + \alpha$$

This simple analysis shows that the XPD of the measurement system introduces a small error of the total power measured by the measurement probe and that the conservation of measured powers is not guaranteed, i.e., the MU based on the XPD can be expressed as:

Equation 2.34-6

$$\text{MU}_{\text{XPD}}[\text{dB}] = 10\log_{10}(1 + \alpha) = 10\log_{10}\left(1 + 10^{\frac{\text{XPD}}{10}}\right)$$

This XPD MU is tabulated for different levels of XPD in [Table 2.34 1](#).

Table 2.34-1 XPD MU for Different XPD Values

XPD [dB]	MU _{XPD} [dB]
-20	0.043
-25	0.014
-30	0.004
-35	0.001
-40	0.000

When the range reference calibration is based on a full matrix-based approach, i.e., all signal paths are calibrated, the conservation of measured powers is guaranteed. As shown in [Figure 2.34 3](#), the polarization-matched signal paths take into account the leakage of power into the cross paths.

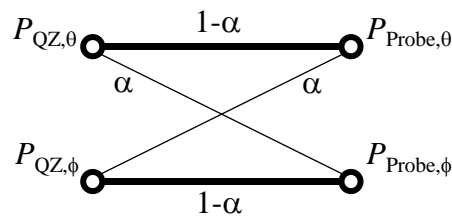


Figure 2.34-3 Calibration Approach Based on Calibrating All Signal Paths

The powers at the measurement probe can now be written as:

Equation 2.34-7

$$P_{\text{Probe},\theta} = (1 - \alpha)P_{\text{QZ},\theta} + \alpha P_{\text{QZ},\phi}$$

Equation 2.34-8

$$P_{\text{Probe},\phi} = (1 - \alpha)P_{\text{QZ},\phi} + \alpha P_{\text{QZ},\theta}$$

The normalized ratio of total powers at measurement probe and the center of the quiet zone is then:

Equation 2.34-9

$$\frac{P_{\text{Probe}}}{P_{\text{QZ}}} = \frac{P_{\text{Probe},\theta} + P_{\text{Probe},\phi}}{P_{\text{QZ},\theta} + P_{\text{QZ},\phi}} = \frac{P_{\text{QZ},\theta} + P_{\text{QZ},\phi}}{P_{\text{QZ},\theta} + P_{\text{QZ},\phi}} = 1$$

This simple analysis now shows that for a matrix-based calibration of all signal paths the XPD of the measurement probe no longer introduces any error and that the conservation of measured powers is guaranteed, i.e., the MU based on the XPD is 0 dB.

The derivation of the XPD MU based on powers is a more straightforward and less complex approach. This shows that the same XPD MU result as derived in Equation 2.34-5 can be derived using electric fields.

The corresponding signal paths are illustrated in Figure 2.34 4.

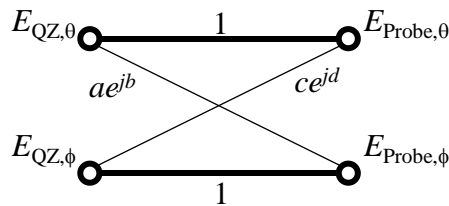


Figure 2.34-4 Signal Paths for Electric Fields (Based on Calibrating the Polarization Matched Signal Paths)

The normalized fields at the measurement probe terminals can then be written as:

Equation 2.34-10

$$E_{\text{Probe},\theta} = E_{\text{QZ},\theta} + ce^{jd} E_{\text{QZ},\phi}$$

Equation 2.34-11

$$E_{\text{Probe},\phi} = E_{\text{QZ},\phi} + ae^{jb} E_{\text{QZ},\theta}$$

The transmission matrix can be defined as H:

Equation 2.34-12

$$\begin{bmatrix} E_{\text{Probe},\theta} \\ E_{\text{Probe},\phi} \end{bmatrix} = H \begin{bmatrix} E_{\text{QZ},\theta} \\ E_{\text{QZ},\phi} \end{bmatrix}$$

with

Equation 2.34-13

$$H = \begin{bmatrix} 1 & ae^{jb} \\ ce^{jd} & 1 \end{bmatrix}$$

The total magnitude component of the electric field including coherence/interference terms at the probe is:

Equation 2.34-14

$$\begin{aligned} E_{\text{Probe},T} &= \sqrt{|E_{\text{Probe},\theta}|^2 + |E_{\text{Probe},\phi}|^2} = \sqrt{|E_{\text{QZ},\theta} + ce^{jd}E_{\text{QZ},\phi}|^2 + |E_{\text{QZ},\phi} + ae^{jb}E_{\text{QZ},\theta}|^2} \\ &= \sqrt{\left[(E_{\text{QZ},\theta} + cE_{\text{QZ},\phi} \cos(d))^2 + (cE_{\text{QZ},\phi} \sin(d))^2 \right] + \left[(E_{\text{QZ},\phi} + aE_{\text{QZ},\theta} \cos(b))^2 + (aE_{\text{QZ},\theta} \sin(b))^2 \right]} \\ &= \sqrt{E_{\text{QZ},\theta}^2 + 2cE_{\text{QZ},\theta}E_{\text{QZ},\phi} \cos(d) + c^2E_{\text{QZ},\phi}^2 \cos^2(d) + c^2E_{\text{QZ},\phi}^2 \sin^2(d) + E_{\text{QZ},\phi}^2 + 2aE_{\text{QZ},\theta}E_{\text{QZ},\phi} \cos(b) + a^2E_{\text{QZ},\theta}^2 \cos^2(b) + a^2E_{\text{QZ},\theta}^2 \sin^2(b)} \\ &= \sqrt{E_{\text{QZ},\theta}^2(1 + a^2) + E_{\text{QZ},\phi}^2(1 + c^2) + 2E_{\text{QZ},\theta}E_{\text{QZ},\phi}(c \cos(d) + a \cos(b))} \end{aligned}$$

When it is assumed that leakage between the two polarization ports of the measurement probe is assumed to be the same, then $a = c = 10\text{XPD}/20$ in Equation 2.34-14. Additionally, it must be assumed that $d=b+\pi$ which guarantees the orthogonality between the two field vectors, i.e., the dot product between the vectors has to be zero. With these assumptions, Equation 2.34-14 will become:

Equation 2.34-15

$$E_{\text{Probe},T} = \sqrt{(E_{\text{QZ},\theta}^2 + E_{\text{QZ},\phi}^2)(1 + a^2)}$$

The normalized ratio of total powers at measurement probe and the center of the quiet zone is therefore:

Equation 2.34-16

$$\frac{P_{\text{Probe}}}{P_{\text{QZ}}} \propto \frac{E_{\text{Probe},T}^2}{E_{\text{QZ},T}^2} = 1 + a^2 = 1 + 10 \frac{2\text{XPD}}{20} = 1 + 10 \frac{\text{XPD}}{10}$$

The derived XPD MU based on electric fields which included the coherence/interference terms in Equation 2.34-16 is the same as in Equation 2.34-6.

The XPD of the measurement system shall be determined from the quality of quiet zone measurements, see CTIA 01.22 [7] at the 7 reference points, P1 through P7, specifically with reference AUT orientations $\gamma=\beta=0^\circ$ for distributed axes systems, CTIA 01.22 [7] at or reference AUT orientations $\beta=\alpha=0^\circ$ for combined-axes systems, elsewhere in that document. Alternatively, it can be determined using a reference antenna optimized for XPD measurements and with the corresponding alignment to achieve optimal polarization matching between the reference and the measurement antenna.

The XPD for each reference point shall be calculated as the ratio of cross-polarized to co-polarized measured powers and the largest XPD from the 7 different reference points shall be used to determine the XPD MU, i.e.,

Equation 2.34-17

$$MU_{XPD}[\text{dB}] = 10\log_{10}(1 + \alpha_{max}) = 10\log_{10}\left(1 + 10^{\frac{XPD_{max}}{10}}\right)$$

where:

Equation 2.34-18

$$XPD_{max}[\text{dB}] = 10\log_{10}\left[\max\left(\frac{P_{cross-pol}}{P_{co-pol}}\bigg|_{P1, \gamma_{rot} = 0^\circ}, \frac{P_{cross-pol}}{P_{co-pol}}\bigg|_{P1, \gamma_{rot} = 90^\circ}, \dots, \frac{P_{cross-pol}}{P_{co-pol}}\bigg|_{P7, \gamma_{rot}}\right)\right]$$

$$= 0^\circ, \frac{P_{cross-pol}}{P_{co-pol}}\bigg|_{P7, \gamma_{rot} = 90^\circ}\bigg]$$

2.35 Phase Center Offset of Calibration Antenna

Gain is defined at the phase center of the antenna. If the phase center of the calibration antenna is not aligned at the center of the set up during the calibration, then there will be uncertainty related to the measurement distance. For more information, see Section 2.9.2.

For DFF systems this uncertainty contribution must be included while this term can be assumed to be zero inside the quiet zone for IFF systems.

2.36 Influence of the Calibration Antenna Feed Path

During the calibration measurement a cable (plus adapters, attenuators) is used to feed the calibration antenna. This uncertainty captures any influence the cable or miscellaneous components (adapters, attenuators, connector, rotary joints) may have on the measurements result. This term can be assessed by repeating measurements while flexing the cables and rotary joints and using the largest difference between the results as the uncertainty.

2.37 Influence of Noise

This contributor describes an offset uncertainty factor caused by a noise floor especially in a case of low SNR. This contributor works as a bias to measured results only to a direction to increase values and thus this shall be included in the uncertainty budget table as a systematic uncertainty. The uncertainty value can be derived by the following equation.

Equation 2.37-1

$$\text{Influence of noise} = 10 * \log\left(1 + 10^{\left(\frac{SNR}{10}\right)}\right)$$

2.38 Systematic Error related to Beam Peak Search

When performing beam peak search measurements, a systematic error shall be taken into account. The value of this contributor depends on the number of measurement grid points.

This measurement uncertainty contributor represents a systematic uncertainty and must be added to the expanded uncertainty and not be root sum squared with contributors described by standard deviation.

2.39 Systematic Error Related to EIS Spherical Coverage

When calculating EIS spherical coverage, a mean error shall be taken into account. The value of this contributor depends on the DL power step size used for the EIS search and the number of measurement grid points.

This measurement uncertainty contributor represents a systematic uncertainty and must not be root sum squared with contributors described by standard deviation.

2.40 Minimum Measurement Distance Considerations

2.40.1 SISO, Anechoic Chamber Test Methodology

Due to the large form factor of some integrated devices, the minimum measurement distance criteria, in particular, the $2D^2/\lambda$ limit specified in Section 1.1 in *CTIA 01.73 [2]* cannot be satisfied on shorter ranges.

To cover the large form factor devices the ATL shall stay within the notebook-sized quiet zone size dimensions detailed in Section 5.4 in *CTIA 01.73 [2]*.

However, an additional standard uncertainty value must be included in the total DUT measurement uncertainty calculation to account for the violation of the far field as identified in [Section 2.9.4.1](#).

2.40.2 SISO, Millimeter Wave Test Methodology

Given that the CATR produces a far field test environment, this contribution is considered to be zero.

2.41 Impact of ATF Pattern Error on TP

This MU element captures the effect of errors in the RSAP and RSARP pattern measurements on the TP measurements. A fixed MU value of 0.2 dB shall be assumed for RTS methodology.

2.42 Impact of Non-Ideal Isolation between Streams in Radiated 2nd Stage

This MU element captures the effect on non-ideal, i.e., infinite, isolation in the radiated 2nd stage of RTS. A fixed MU value of 0.2 dB shall be assumed for RTS methodology.

2.43 Multiple Measurement Antennas

This contributor describes the uncertainty caused by switching multiple measurement antennas either mechanically or electrically.

Section 3 Assessment of Uncertainty Values using Simulation Tools (Normative)

3.1 Introduction

Uncertainty assessments are always relative evaluations and therefore well suited for numerical simulation tools which provide the most appropriate technique to compare different configurations. It can be guaranteed that the relative accuracy is significantly better than 0.1 dB. The simulation tools can be used for Type B and Type A evaluations. Type A evaluations require sufficient computational resources and scripting of the input file to satisfy the required random modifications. Type B evaluations are straightforward and consider only the average and both maximum bounds of the tolerance.

The purpose of this appendix is to describe the concept of uncertainty assessment using simulation tools including the validation of the tool and numerical evaluation procedure.

3.2 Requirements for the Simulation Software

The basic requirements of the simulation software must be the following:

- Import of mobile phone CAD data (typically, >500 parts) as well as head/hand/forearm phantoms and fixture data
- Accurate simulation of mobile phones with homogenous head, hand and forearm phantoms including effect on impedance, efficiency, and performance
- Position of mobile phone and phantoms with high precision
- Evaluation of end points specified in Section 2.13
- Scripting abilities

3.3 Simulation Software Validation

The simulation software should be validated by the manufacturers according to the following:

- Checking the correct evaluation of the end points specified in Section 2.13 of dipoles
- Checking the correct evaluation of the end points specified in Section 2.13 of dipoles with different locations of the absorbing boundary conditions (ABC) if applicable
- Computation of the benchmark examples listed in *IEEE P1528.1™/D1.0 [18]* and *IEEE P1528.4™/D1.0 [19]* following the procedure defined in the same documents
- Computation of the benchmark examples of SAM phantom, as defined by Beard et. al using different meshing densities

3.4 Phone Validation

The uncertainty evaluation requires different mobile phone models (see Section 1).

- The phone models including effects of back scattering on the impedance shall be validated by SAR distribution or near-field free space comparison (distance to the surface of the phone less than 20 mm) for different distances from the phone, e.g., 5 mm, and 10 mm. If the deviation of all distances with respect to the peak and pattern (gamma method comparison) is less than 15%, the phone can be considered validated.
- The phone models shall be validated by TRP and efficiency comparisons.

3.5 Computation of the Uncertainty for Type B Evaluation

Type B evaluations are straightforward. Only the average and both maximum bounds of the tolerance will be considered, whereas, the rectangular distribution is assumed. These cases are computed with the previously validated code and for different phone models if required. The difference in the end points specified in [Section 2](#) compared to the standard case will be compared and the maximum will be used for the uncertainty budget.

3.6 Computation of the Uncertainty for Type A Evaluation

Although Type A evaluations require more powerful tools than Type B evaluations, they are more reliable. A parameter distribution is experimentally determined or predicted. These parameters are then scripted in the software tool and the magnitude of the parameters is randomly assigned and compliant with the determined distribution. The difference in the end points specified in [Section 2](#) is evaluated for each simulation case in which an appropriate statistical analysis shall be performed.

3.7 Numerical Evaluation of Head and Hand Phantom Fixtures Uncertainty

The numerical evaluation compares the differences between the end points specified in [Section 2](#) with and without fixtures and mounting structures. Type A and B evaluations shall be applied, the highest of which shall be used.

The evaluation procedure requires the existence of CAD model files of the different phone models, head and hand phantoms, and their fixtures. A proposed and recommended procedure for importing and preprocessing the phone model can be found in *IEEE P1528.3™/D2.0* [\[18\]](#).

1. Import antenna and PCB of the handset model into simulation software.
2. Model source by implementing a feed gap or other source model.
3. Import the remaining parts in order of importance and set material parameters.
4. Validate the phone in free-space by comparing near-field according to [section 3.5](#).
5. Import models of the head and hand phantoms into the same model space and set material parameters according to *CTIA 01.72* [\[12\]](#).
6. Position the phone with respect to the head and hand phantoms according to the procedure defined in *CTIA 01.71* [\[4\]](#).
7. Import models of head and hand phantom fixtures and mounting structures into the same model space.
8. Position them to operate as fixture and/or mounting structures and set material parameters.
9. Perform the initial simulation for each frequency band and evaluate the end points specified in [section 2.13](#).
10. Without changing any simulation settings and discretizations, repeat step 9 without fixtures and mounting structures.

3.8 Numerical Evaluation of Device Positioning Uncertainty

Numerical evaluation of device positioning uncertainty is a Type A uncertainty analysis which is conducted using high-end simulation tools supporting scripting of mechanical positioning.

The first step of the procedure, as described in [Section 2.13.2.5.1](#), is conducted without measurement. A mechanical position matrix is derived for which the analysis is conducted following the procedures described in [Section 2](#).

1. Import antenna and PCB of the device model into simulation software.
2. Model source by implementing a feed gap or other source model.
3. Import the remaining parts in order of importance and set material parameters.
4. Validate the device in free-space by comparing near-field according to [section 3.5](#).

5. Import models of the head, hand or forearm phantoms into the same model space and set material parameters according to *CTIA 01.72* [12].
6. Position the device with respect to the phantoms according to the procedure defined in *CTIA 01.71* [4].
7. Import models of phantom fixtures and mounting structures into the same model space.
8. Position them to operate as fixture and/or mounting structures and set material parameters.
9. Perform the initial simulation for each frequency band and evaluate the end points specified in section 2.13.
10. Using scripting features of simulation software, generate different simulation projects according to the mechanical position matrix. Each project has to use the same simulation settings and discretization of the device as in the initial simulation.
11. Repeat step 1 to step 10 for each phone model.
12. Performance of the statistical evaluation of the simulated data per device for the end points specified in section 2.13. The largest standard deviation shall be used for the uncertainty budget with a degree of freedom equal to $M/n - 1$, where M is the total number of simulations, and n is the number of DUTs used in the simulations. If there are a sufficient number of simulations, then a more sophisticated ANOVA analysis can be performed.

3.9 Numerical Evaluation of Head, Hand and Forearm Phantom Shape Uncertainty

The head phantom shape uncertainty is the effect of the production tolerances of the inner and outer surfaces of the shell. The hand and forearm phantom shape uncertainty results from the production tolerance of the outer surface of the phantom. If the tolerance in both case is not within 2% from the specified dimensions in the CAD files, then a numerical evaluation must be conducted to determine the uncertainty.

The numerical evaluation procedure requires the existence of CAD model files of the original of head/hand/forearm phantoms and the phantoms with shapes deviated from the original. Following the proposed and recommended procedure in *IEEE P1528.1™/D1.0* [18] *IEEE P1528.4™/D1.0* [19] and *IEEE P1528.3™/D2.0* [20] the device models are initially simulated with the original head, hand and forearm phantoms and the end points specified in section 2.13. are evaluated for each frequency band. The simulations are then repeated after the original models are replaced with the deviated models. The end points specified in section 2.13. obtained in both cases are compared to determine the uncertainty value due to the tolerance of phantom shape.

3.10 Numerical Evaluation of Head Phantom Support Material Uncertainty

The head phantom support material uncertainty results from the supporting dielectric structures of the head phantom. If the effect of the supporting material on the end points specified in section 2.13 cannot be neglected, then a numerical evaluation must be conducted.

The numerical evaluation compares the differences between the end points specified in section 2.13 with and without head phantom support/mounting structures. Following the proposed and recommended procedure in *IEEE P1528.1™/D1.0* [18] *IEEE P1528.4™/D1.0* [19] and *IEEE P1528.3™/D2.0* [20] the phone models are initially simulated with the original head phantom without supporting material and the end points specified in section 2.13 are evaluated for each frequency band. The simulations are then repeated after the supporting/mounting structure is added to the head phantom. The end points specified in section 2.13 obtained in both cases are compared to determine the uncertainty value due to the head phantom supporting/mounting structure.

Section 4 Lab Repeatability Evaluation (Normative)

The laboratory repeatability evaluation is a check of the repeatability of the OTA evaluations; it is recommended that the evaluation be conducted once per year or more frequently, depending on any changes in the staff performing the OTA test.

The repeatability evaluation can be conducted within a short period or distributed over the year. It shall be conducted for the following endpoints:

- Total Radiated Power (TRP)
- Total Isotropic Sensitivity (TIS)
- Power radiated over $\pm 45^\circ$ near the Horizon (NHPRP ± 45)
- Power radiated over $\pm 30^\circ$ near the Horizon (NHPRP ± 30)

A Type A uncertainty analysis consists of the following steps and shall be repeated for each person who may perform tests (T_x) using at least two different DUTs (D_x). The DUTs can be reference phones which have been verified to be stable.

All the phones used in the study shall be characterized and documented.

1. Shut down all equipment and unmount head and phone.
2. Set up and verify the system is functioning properly as usually performed before a test
3. Select the measurement order of devices $D_x (D_1 \dots D_n)$ operating at test frequencies $f_x (f_1 - f_i)$ and measured by the technicians $T_x (T_1 \dots T_m)$, where n shall be larger than 3 and equally divided between monoblock and fold phones with at least one antenna at the bottom of the device.
4. Test person T_x mount device D_x in the hand phantom and at the head phantom.
5. Determine TRP/NHPRP/UHRP/PGRP for the selected frequencies.
6. The same test person T_x mounts Device D_{x+1} in the hand and at the head and repeat steps 3 and 4.
7. Change technicians and repeat steps 1 and 5 until all technicians have positioned each phone at least once and at least 10 evaluations have been performed for each device, i.e., number of measurements M shall be equal to or larger than 40 times the number of test frequencies
8. Performance of the statistical evaluation of the measured data per device for TRP, NHPRP $\pm 30^\circ$, NHPRP $\pm 45^\circ$. The largest standard deviation shall be used for the uncertainty budget with a degree of freedom equal to $M/n - 1$. If there are a sufficient number of measurements then a more sophisticated ANOVA analysis can be performed.

Determine the distribution of the results and the standard deviations for all assessments. The distribution should be close to Gaussian and none of standard deviation should exceed the uncertainty of the laboratory repeatability as determined according to CTIA 01.20 [5].

Appendix A Revision History

Date	Version	Description
February 2022	4.0.0	<p>Initial release</p> <p>Contents moved from SISO OTA test plan. Implementation of the following contributions:</p> <ul style="list-style-type: none"> • Addition of Wide Hand Phantoms • Addition of testing Chest-Worn Devices on Chest Phantom • Addresses the issues related to Ripple Testing with Large Dipoles • Revision of Range Reference Ripple, including clarifying the method used to calculate the term and revising text for ripple based and advanced calibrations • Update to Minimum Range Length Requirements (for historical purposes, removal of following reference: Huff, J.D, et al., "Using Spherical Near-Field Transforms to Determine the Effects of Range Length on the Measurement of Total Radiated Power", 34th Proceedings of the Antenna Measurement Techniques Association (AMTA-2012), Bellevue, WA, October 2012) <p>Contents moved from MIMO Multi-Probe Anechoic Chamber Test Plan</p> <p>Contents moved from SISO Millimeter Wave Test Plan. Harmonize the coverage factor in the mmwave test plan (1.96) to that in the SISO test plan (2.0).</p> <p>Contents moved from Wireless Large Form Factor Device OTA Performance test plan and added Unknown K factor for Small Form Factor DUTs in Section 2.8.3.</p> <p>Addition of terms related to Test Methodology MIMO Radiated Two Stage</p>
December 2022	5.0.0	<p>Section 2:</p> <ul style="list-style-type: none"> • Updates to TBDs and some variables in Section 2.13.4 • Added Section 2.13.5, Ankle Uncertainties
March 2023	6.0.0	<p>Section 2.21:</p> <ul style="list-style-type: none"> • Updates to measurement uncertainty related to TRP TIS measurement grid spacing. • Added 2.43 Multiple Measurement Antennas • Corrected Equation 2.9.3.2-2

September 2023	6.0.1	<p>Section 1:</p> <ul style="list-style-type: none"> • Section 1.3, Changed all references to [11] to [4] throughout the document, and then removed reference [11] which was a duplicate of reference [4]. <p>Section 2:</p> <ul style="list-style-type: none"> • Table 2.13.2.6-1 was updated to remove references to the hand only measurement uncertainties. • Table 2.13.2.7-1 was updated. • Added equations in Section 2.13.3.1 for clarity. • Corrected Equation 2.13.3.2-1 and some references in Section 2.13.3.2. • Corrected a figure reference in Section 2.13.3.2. • Updated some equation references in Table 2.13.3.4-1. • Added equations in Section 2.13.4.1 for clarity. • Updated some equation references and table references in Section 2.13.4.2. • Updated Table 2.13.4.3-1. • Added equations in Section 2.13.5.1 for clarity. • Updated some equation references and table references in Section 2.13.5.2. • Updated Table 2.13.5.3-1.
-------------------	-------	--